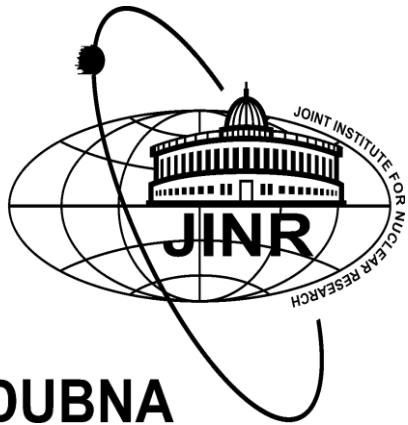


Supporting the existence of the QCD critical point by compact star observations



David Álvarez Castillo



COMPACT STARS IN THE QCD PHASE DIAGRAM IV

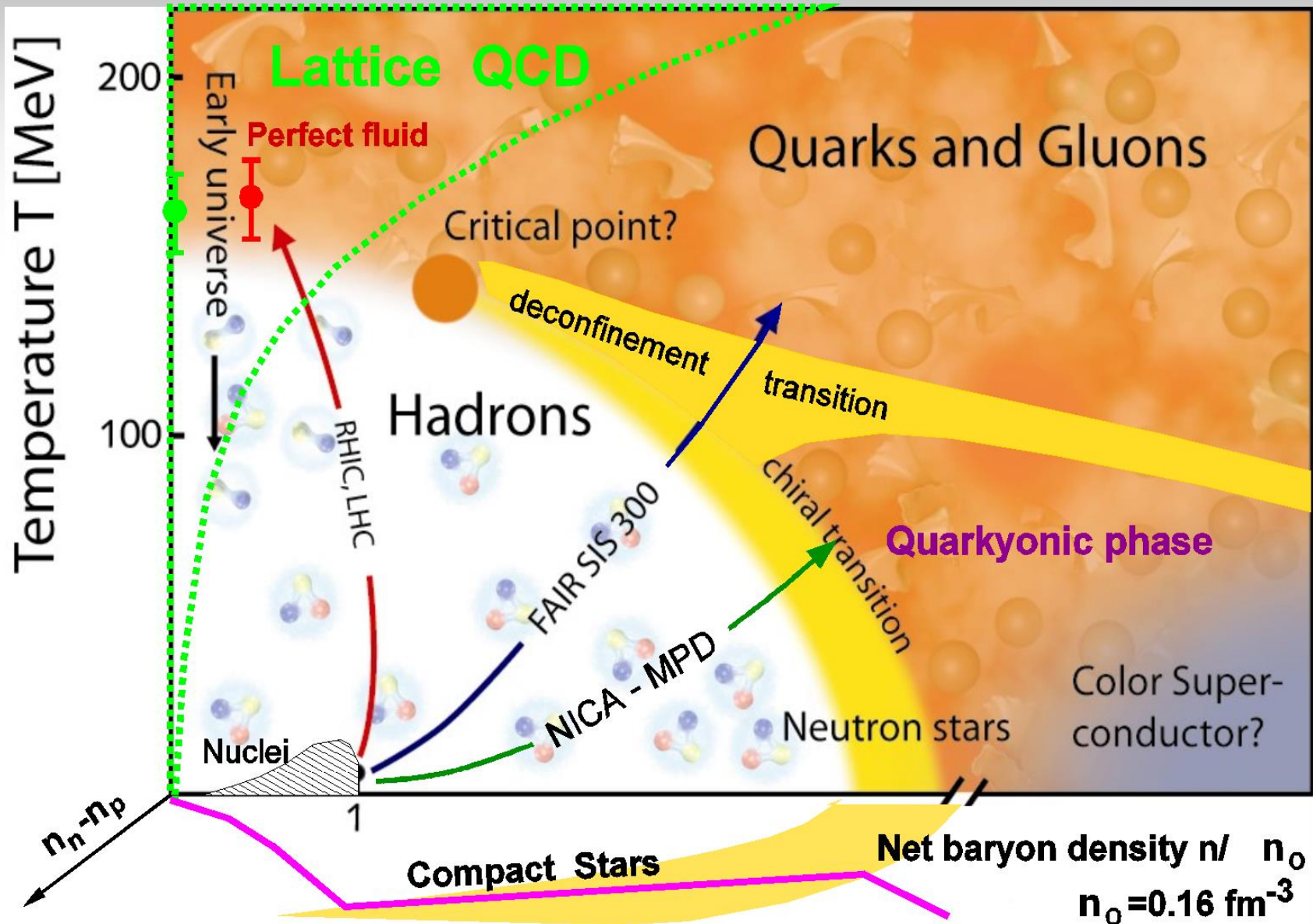
PREROW, GERMANY

September 2014

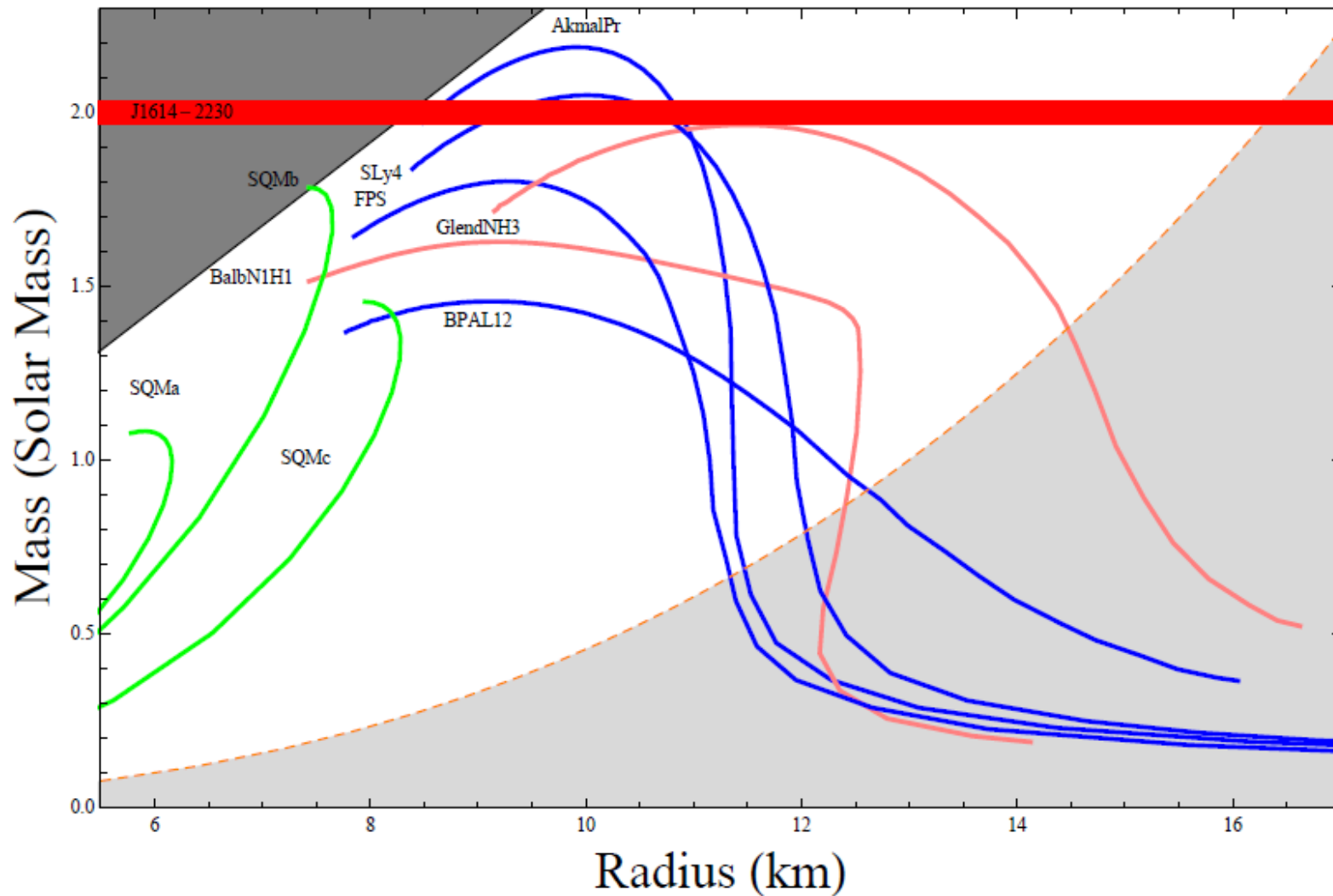
Outline

- Introduction to the QCD phase diagram and compact stars
- First order phase transition and deconfinement in compact stars: masquerade problem vs neutron star twins.
- Bayesian Analysis of hybrid star models.
- Astrophysical implications and perspectives

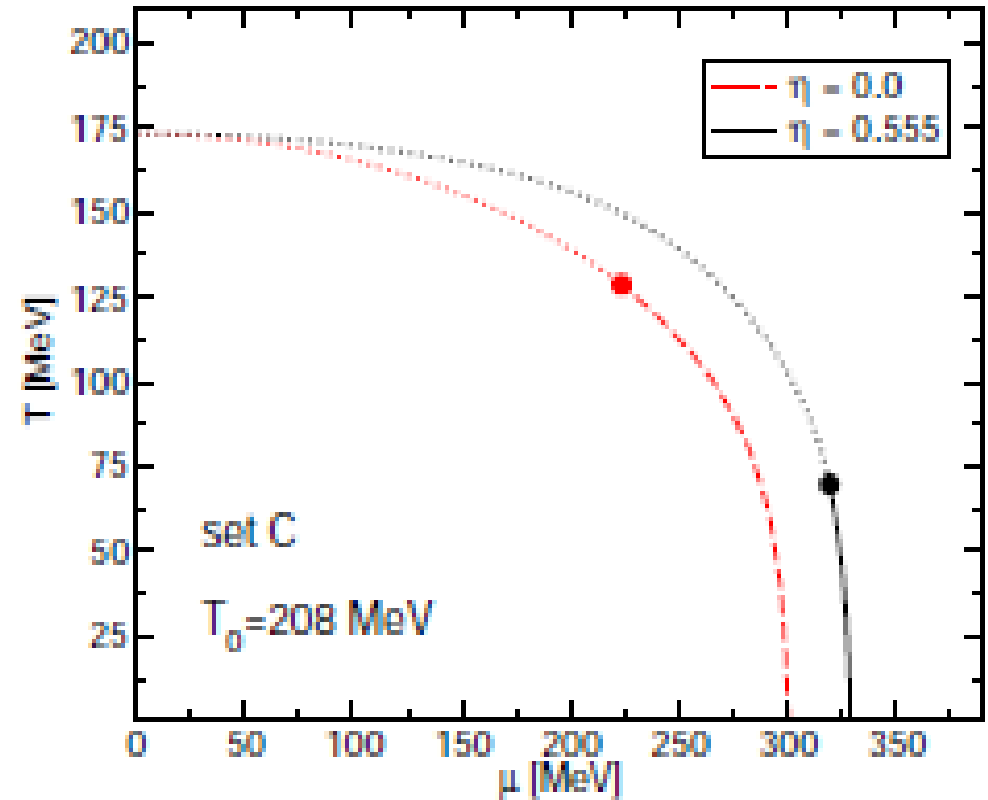
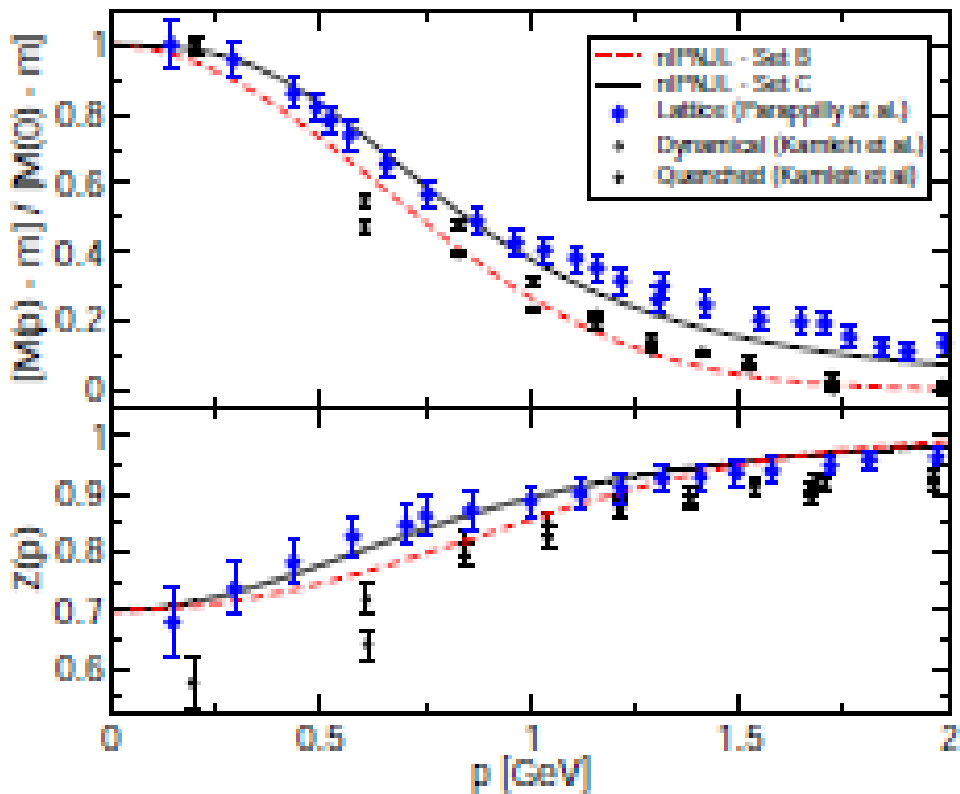
Critical End Point in QCD



Mass vs. Radius Relation



A QCD-based hybrid EoS

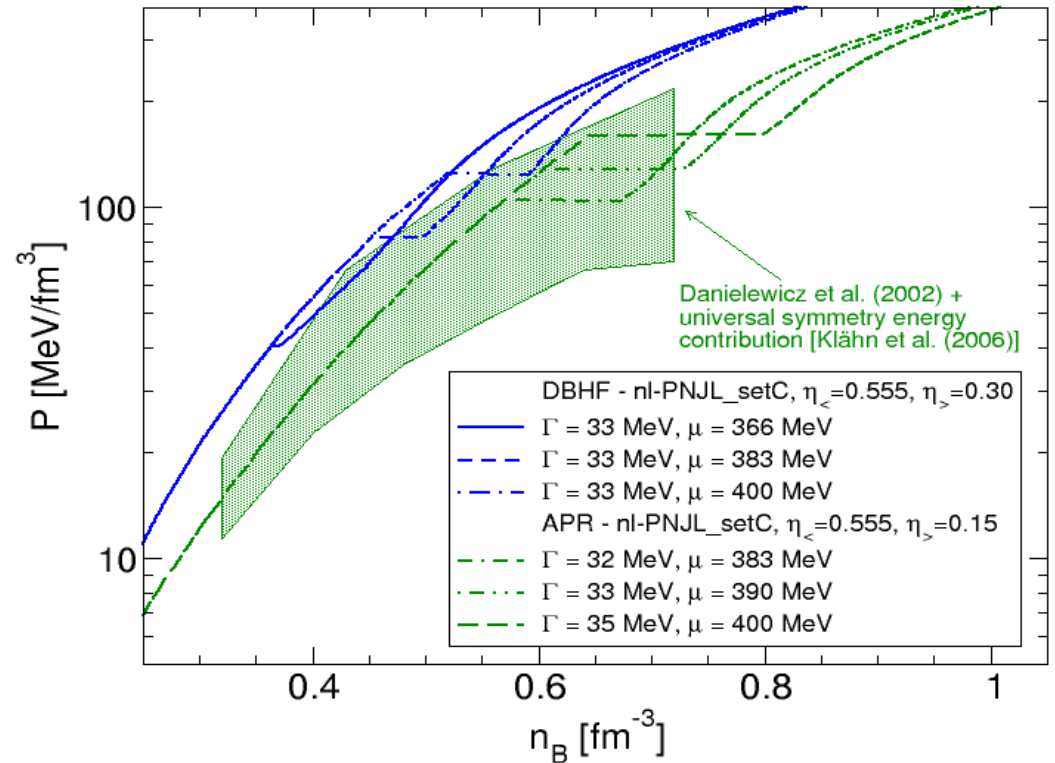
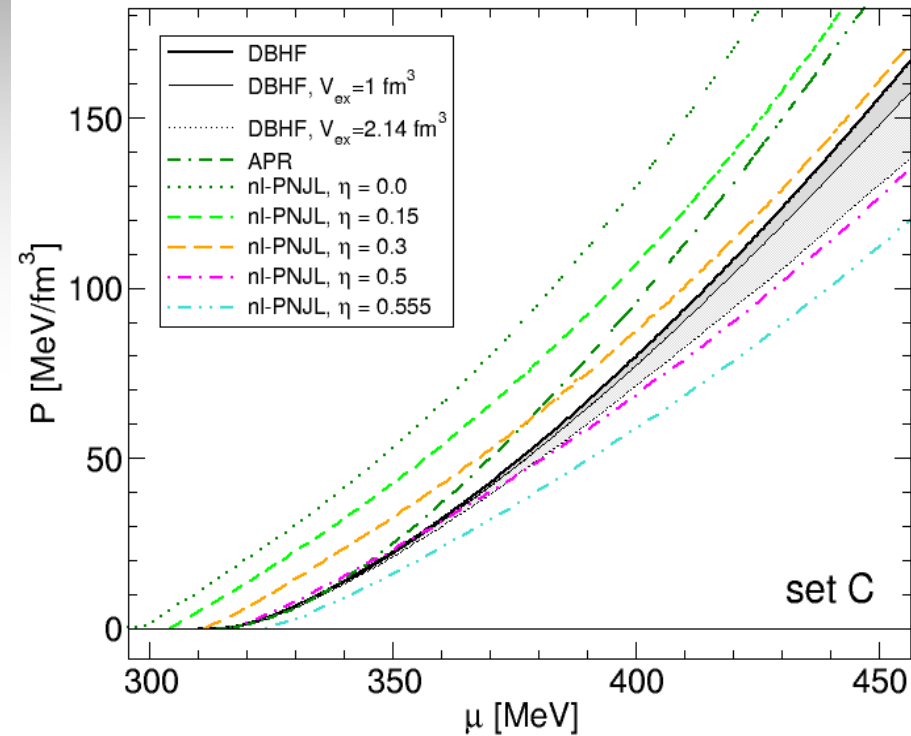


Blaschke, Alvarez-Castillo, Benic, Contrera, Lastowiecki

arXiv:1302.6275

- Formfactors of the nonlocal chiral quark model fixed by comparison with $M(p)$ and $Z(p)$ from lattice QCD calculations of the quark propagator [Parapilly et al. PRD 73 (2006)]
- Vector coupling strength adjusted to describe the slope of the pseudocritical temperature
In accordance with lattice QCD [Kaczmarek et al., PRD 83 (2011) 014504]
- CEP does not vanish !! Controversial discussion, see Hell et al., arxiv:1212.4017 (2012)

A QCD-based hybrid EoS



- for strong vector coupling nuclear matter is stable at low densities
- for small vector coupling quark matter is stable at high densities
- for intermediate couplings → masquerade problem [Alford et al. ApJ 629 (2005) 969]

Here:

(A) Maxwell construction

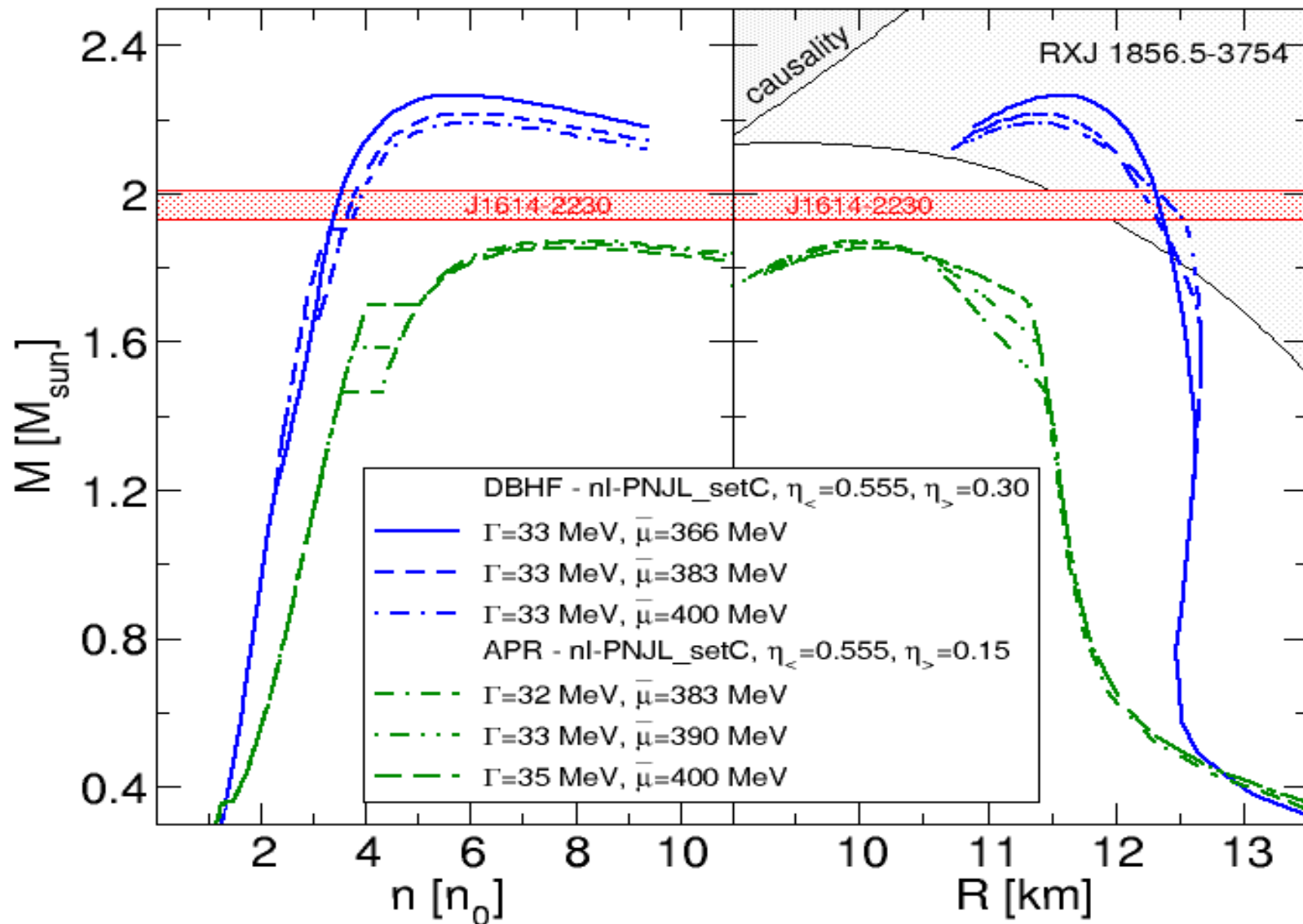
(B) mu-dependent vector coupling:

$$P_Q(\mu_c) = P_H(\mu_c) \quad \text{H = DBHF, APR; Q = nl-PNJL}$$

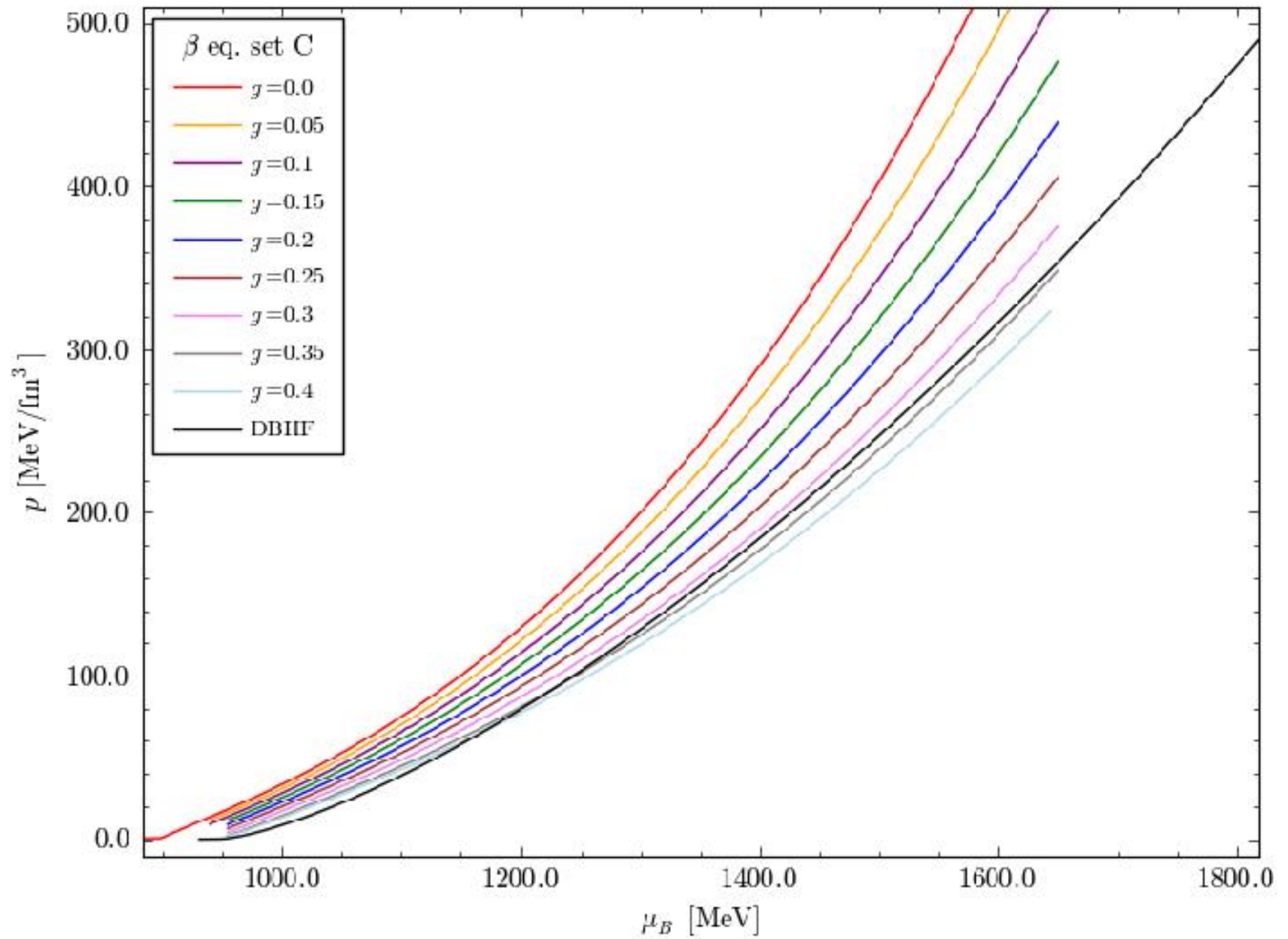
$$P_Q(\mu) = P(0, \mu; \eta_<) f_<(\mu) + P(0, \mu; \eta_>) f_>(\mu),$$

$$f_\xi(\mu) = \frac{1}{2} \left[1 \mp \tanh \left(\frac{\mu - \bar{\mu}}{\Gamma} \right) \right].$$

Result 1: hybrid stars fulfill Demorest and RXJ1856

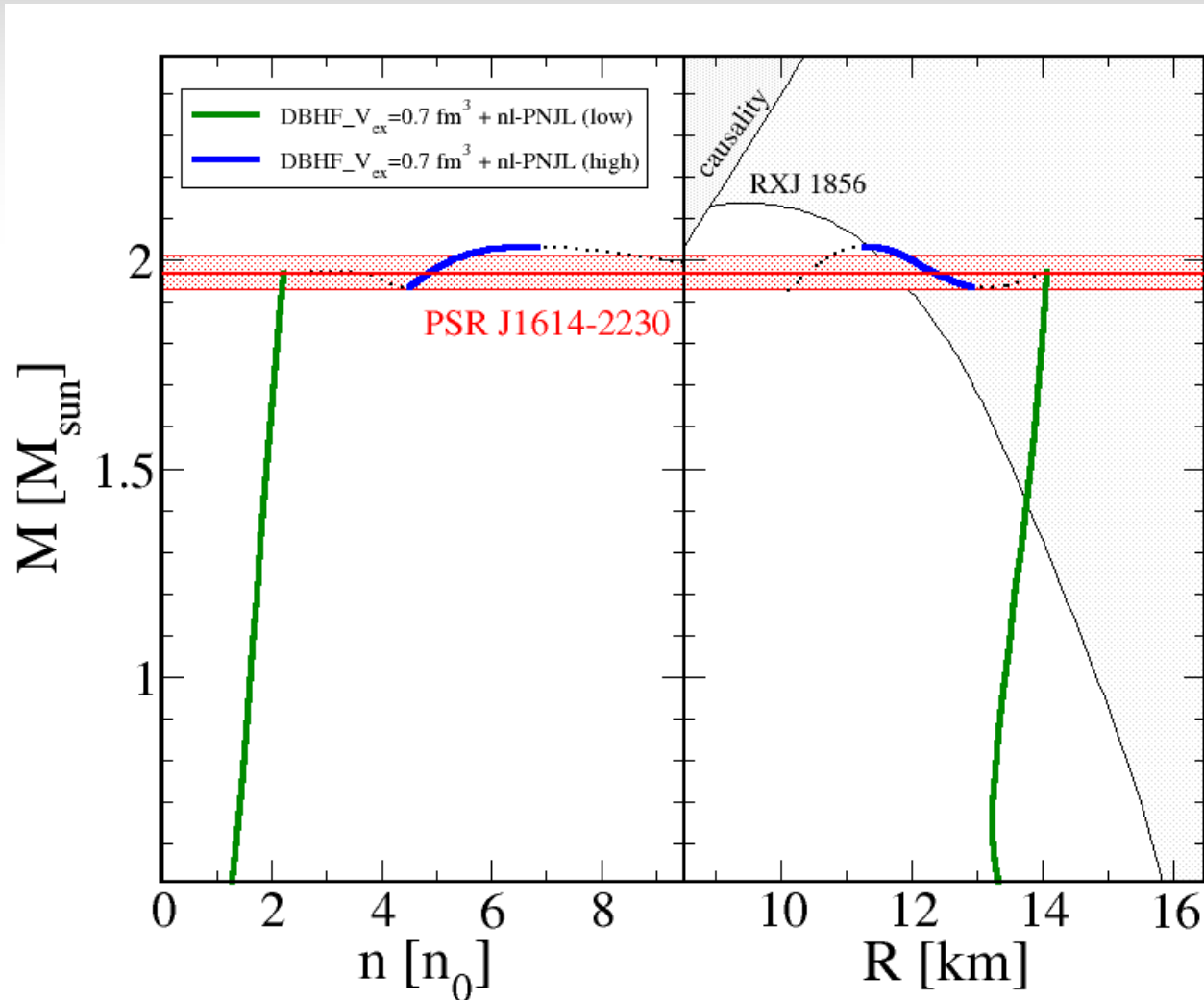


Masquerades

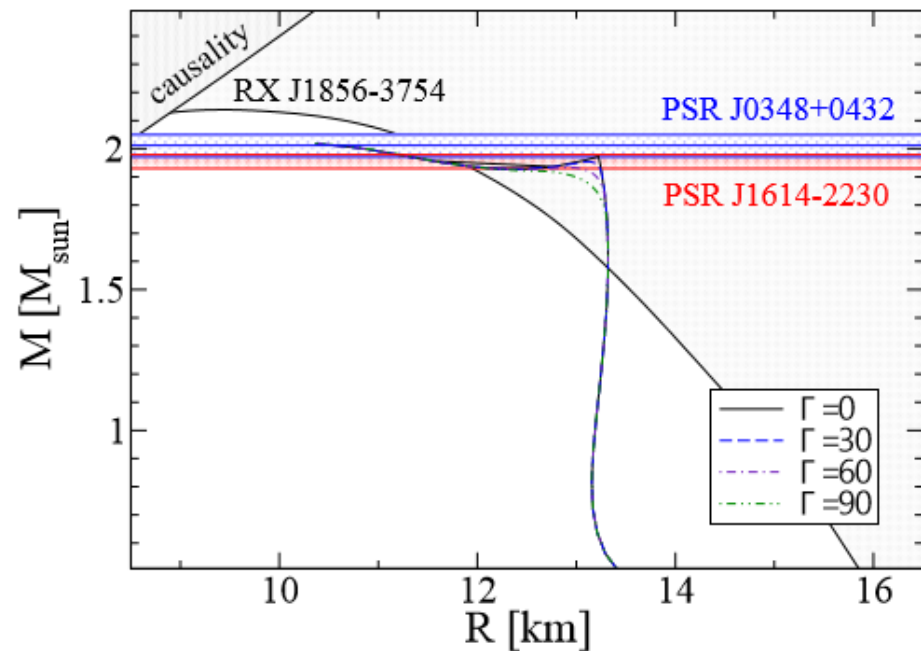
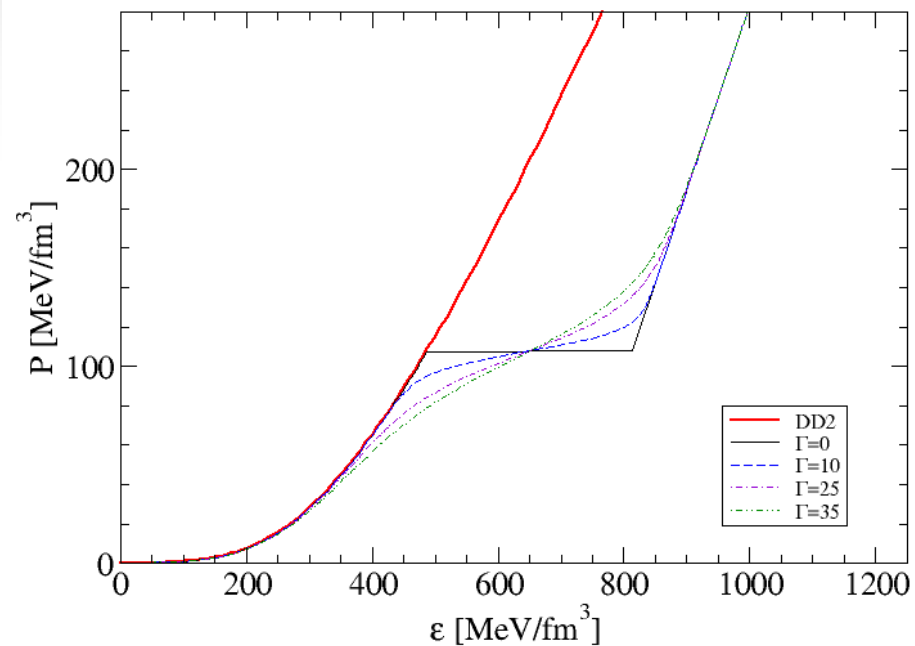


Proving the CEP with Compact Stars

Third family (disconnected branch)



Pasta phases in hybrid stars



$$\epsilon_{\text{pasta}}(p) = \epsilon_h(p) * f_{<}(p) + \epsilon_q(p) * f_{>}(p),$$

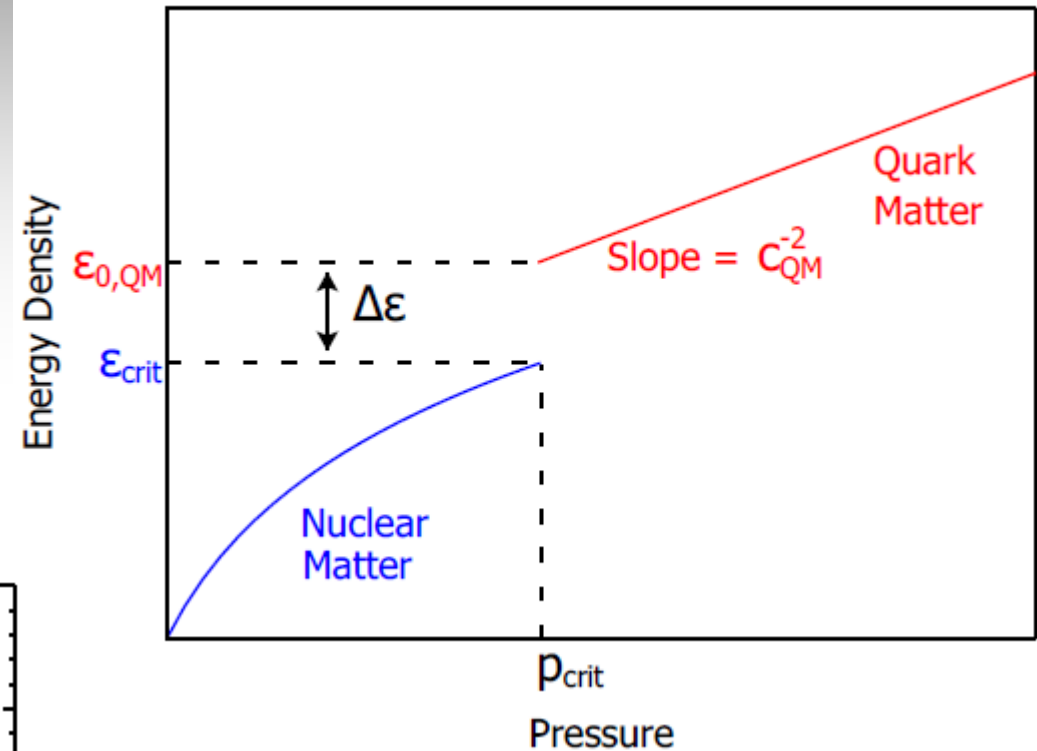
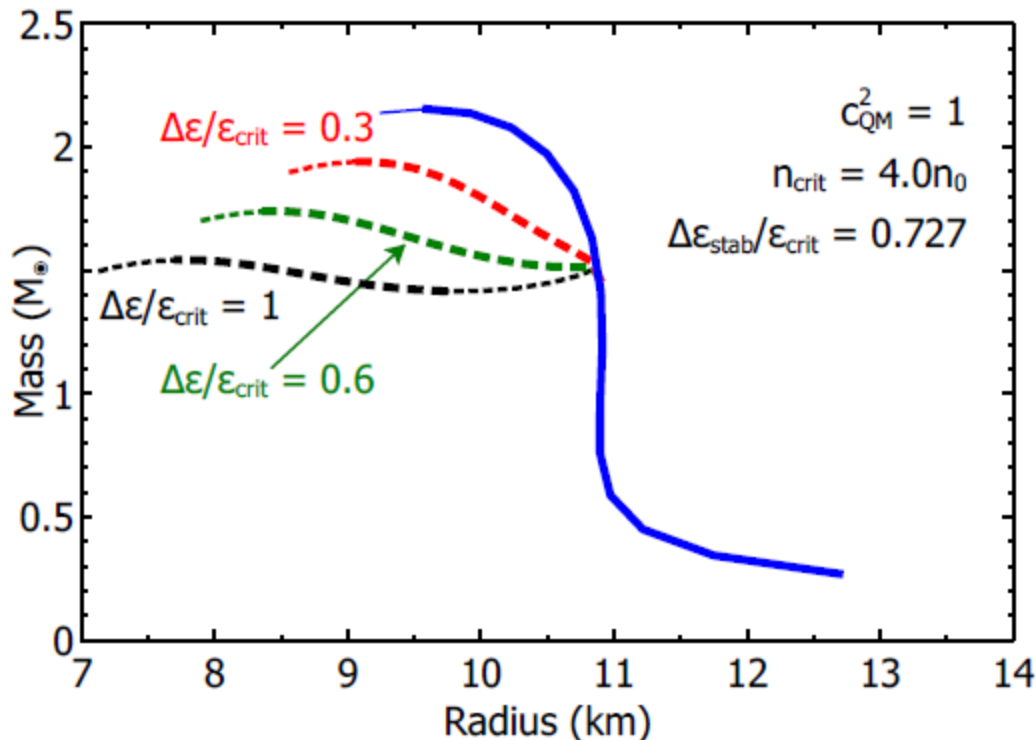
$$f_{<}(p) = \frac{1}{2} \left(-\tanh\left(\frac{p - \bar{p}}{\Gamma}\right) + 1 \right),$$

$$f_{>}(p) = \frac{1}{2} \left(\tanh\left(\frac{p - \bar{p}}{\Gamma}\right) + 1 \right),$$

Neutron Star Twins and the AHP scheme

Alford, Han, Prakash, arxiv:1302.4732

First order PT can lead to a stable branch of hybrid stars with quark matter cores which, depending on the size of the “latent heat” (jump in energy density), can even be disconnected from the hadronic one by an unstable branch → “**third family of CS**”.



Measuring two **disconnected populations** of compact stars in the M-R diagram would be the **detection of a first order phase transition** in compact star matter and thus the indirect proof for the existence of a **critical endpoint (CEP) in the QCD phase diagram!**

Baryon substructure effect (EVA)

Excluded volume approximation (EVA):

$$p_{\text{ex}}(\mu, T) = p(\tilde{\mu}, T), \quad \tilde{\mu} = \mu - v_0(\mu, T)p_{\text{ex}}(\mu, T)$$

$$n_{\text{ex}}(\mu, T) = \frac{\partial p_{\text{ex}}}{\partial \mu} = \frac{\partial \tilde{\mu}}{\partial \mu} \frac{\partial p(\tilde{\mu}, T)}{\partial \tilde{\mu}} = \left[1 - v_0 n_{\text{ex}}(\mu, T) - \frac{\partial v_0}{\partial \mu} p_{\text{ex}}(\mu, T) \right] n(\tilde{\mu}, T)$$

Thermodynamic consistency:

$$\epsilon_{\text{ex}}(\mu, T) = -p_{\text{ex}}(\mu, T) + \mu n_{\text{ex}}(\mu, T) + T s_{\text{ex}}(\mu, T)$$

Parametrization of excluded volume with nonlinear dependence on the chemical potential:

$$v_0(\mu, T) = (4\pi/3)r^3(\mu), \quad r^3(\mu) = r_0 + r_1(\mu/\mu_c)^2 + r_2(\mu/\mu_c)^4$$

NJL model with multiquark interactions

$$\mathcal{L} = \bar{q}(i\cancel{\partial} - m)q + \mu_q \bar{q}\gamma^0 q + \mathcal{L}_4 + \mathcal{L}_8, \quad \mathcal{L}_4 = \frac{g_{20}}{\Lambda^2} [(\bar{q}q)^2 + (\bar{q}i\gamma_5\tau q)^2] - \frac{g_{02}}{\Lambda^2} (\bar{q}\gamma_\mu q)^2,$$

$$\mathcal{L}_8 = \frac{g_{40}}{\Lambda^8} [(\bar{q}q)^2 + (\bar{q}i\gamma_5\tau q)^2]^2 - \frac{g_{04}}{\Lambda^8} (\bar{q}\gamma_\mu q)^4 - \frac{g_{22}}{\Lambda^8} (\bar{q}\gamma_\mu q)^2 [(\bar{q}q)^2 + (\bar{q}i\gamma_5\tau q)^2]$$

Meanfield approximation: $\mathcal{L}_{\text{MF}} = \bar{q}(i\cancel{\partial} - M)q + \tilde{\mu}_q \bar{q}\gamma^0 q - U,$

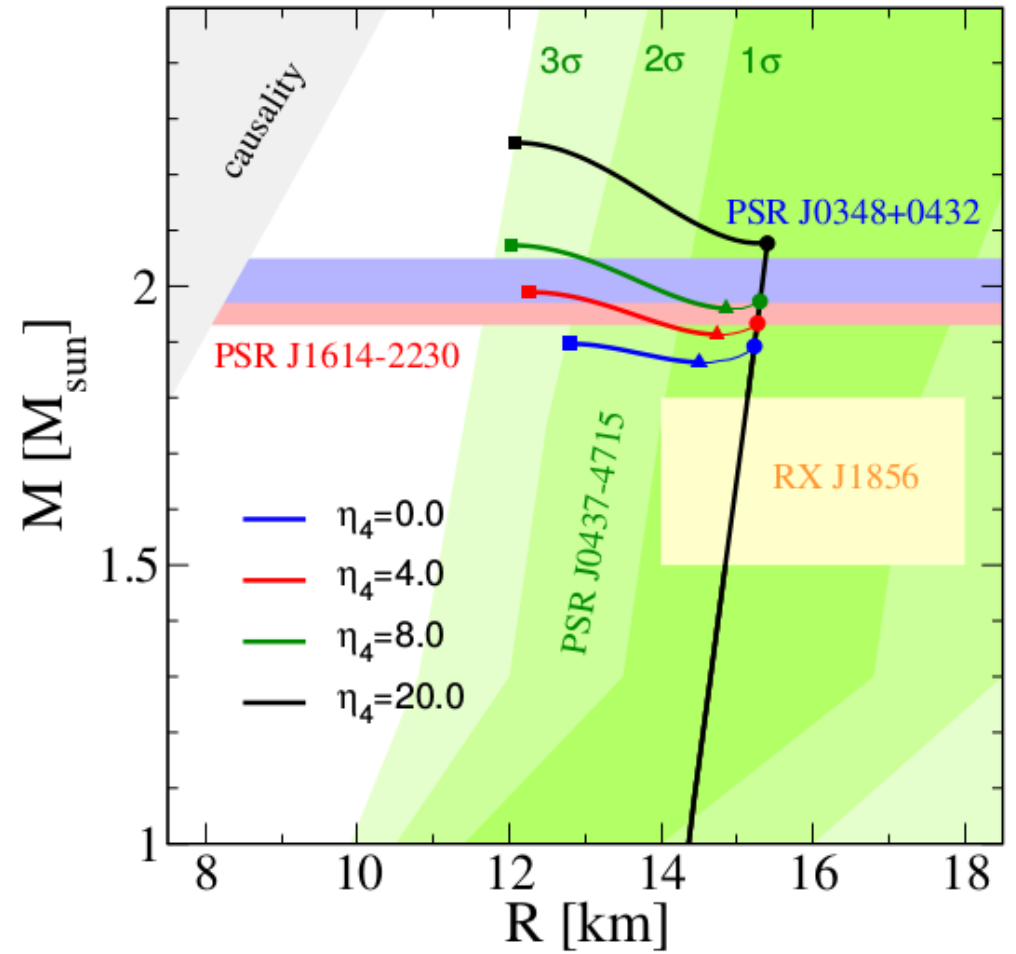
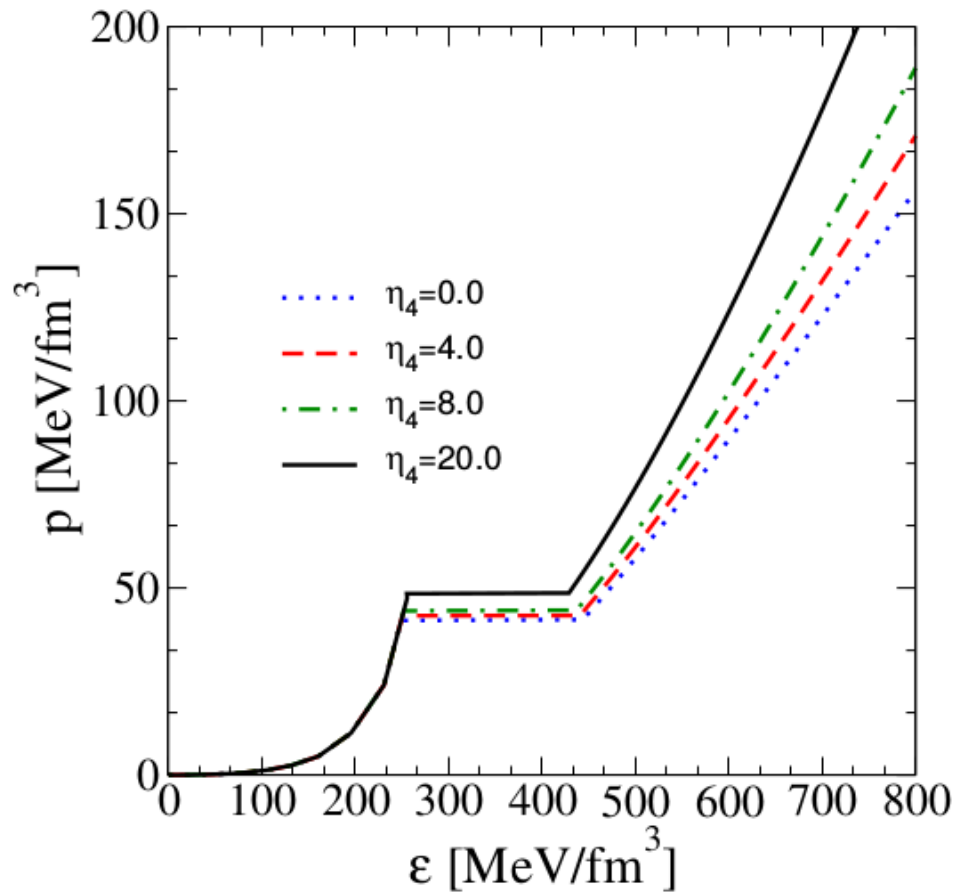
$$M = m + 2\frac{g_{20}}{\Lambda^2} \langle \bar{q}q \rangle + 4\frac{g_{40}}{\Lambda^8} \langle \bar{q}q \rangle^3 - 2\frac{g_{22}}{\Lambda^8} \langle \bar{q}q \rangle \langle q^\dagger q \rangle^2,$$

$$\tilde{\mu}_q = \mu_q - 2\frac{g_{02}}{\Lambda^2} \langle q^\dagger q \rangle - 4\frac{g_{04}}{\Lambda^8} \langle q^\dagger q \rangle^3 - 2\frac{g_{22}}{\Lambda^8} \langle \bar{q}q \rangle^2 \langle q^\dagger q \rangle,$$

$$U = \frac{g_{20}}{\Lambda^2} \langle \bar{q}q \rangle^2 + 3\frac{g_{40}}{\Lambda^8} \langle \bar{q}q \rangle^4 - 3\frac{g_{22}}{\Lambda^8} \langle \bar{q}q \rangle^2 \langle q^\dagger q \rangle^2 - \frac{g_{02}}{\Lambda^2} \langle q^\dagger q \rangle^2 - 3\frac{g_{04}}{\Lambda^8} \langle q^\dagger q \rangle^4.$$

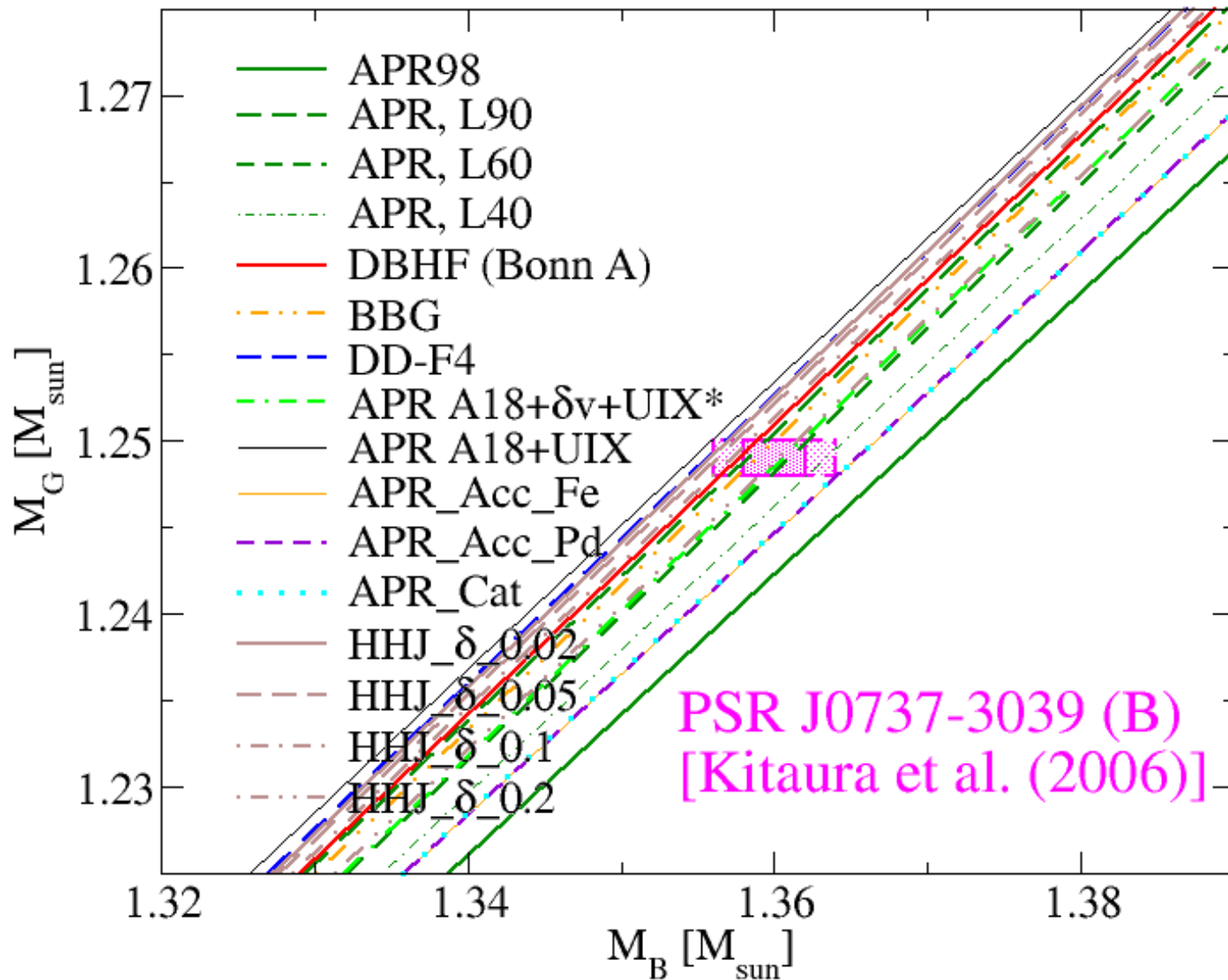
Thermodynamic Potential:

$$\Omega = U - 2N_f N_c \int \frac{d^3 p}{(2\pi)^3} \left\{ E + T \log[1 + e^{-\beta(E - \tilde{\mu}_q)}] + T \log[1 + e^{-\beta(E + \tilde{\mu}_q)}] \right\} + \Omega_0$$



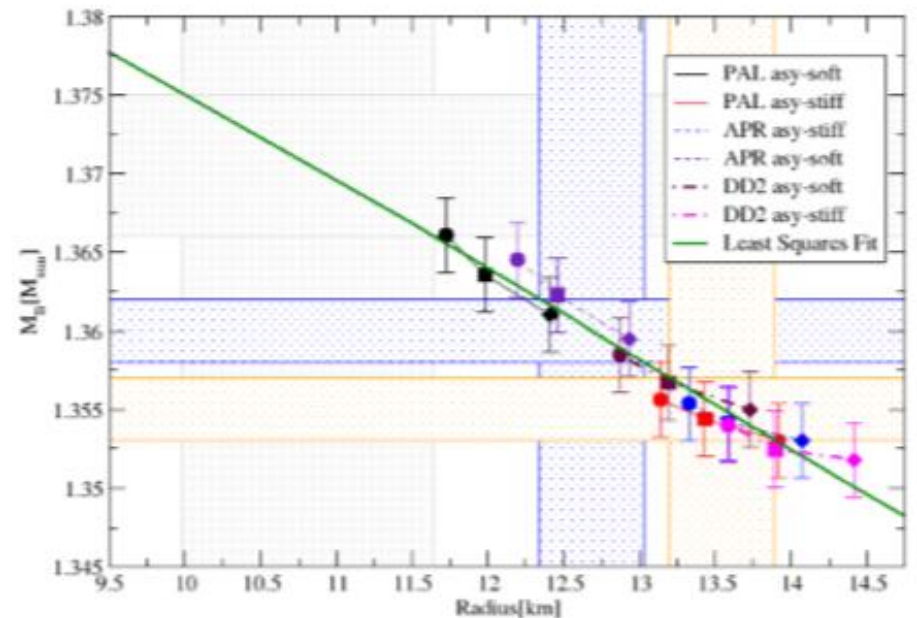
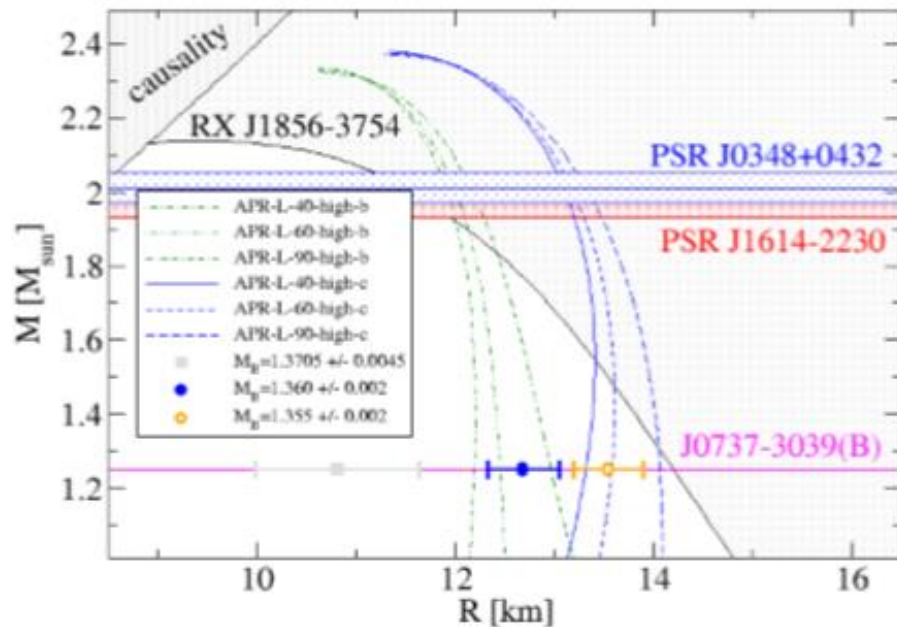
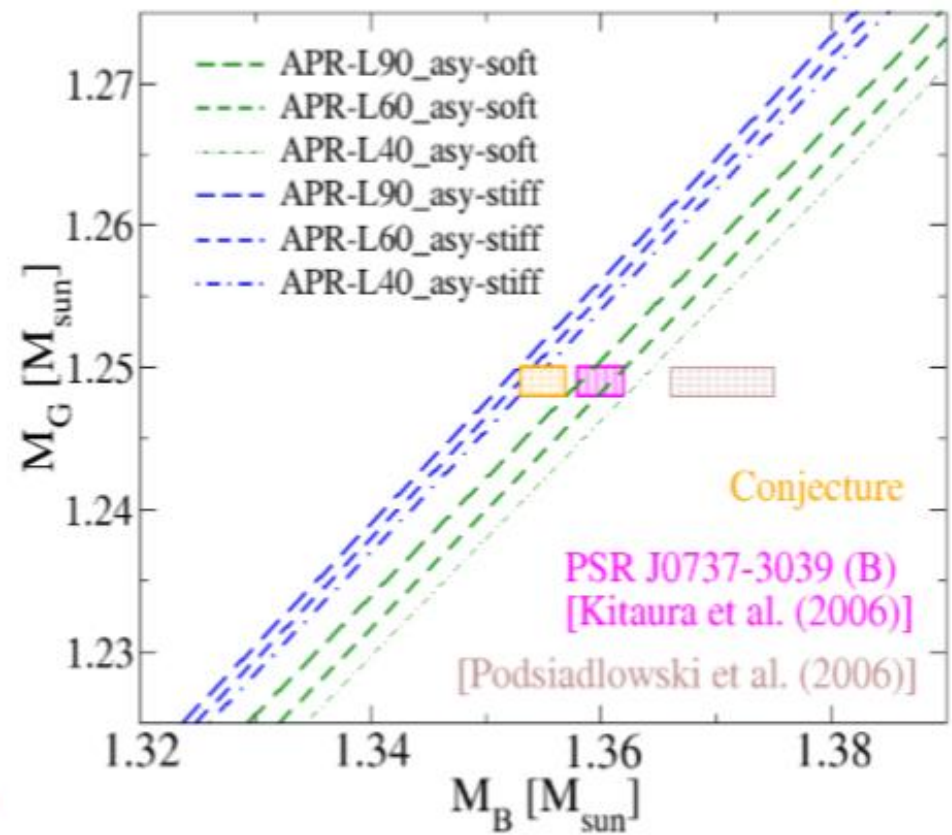
Benic, Blaschke, Alvarez-Castillo, Fischer, in progress (2014)

Baryonic Mass



Neutron star EoS: radius from M_B ?

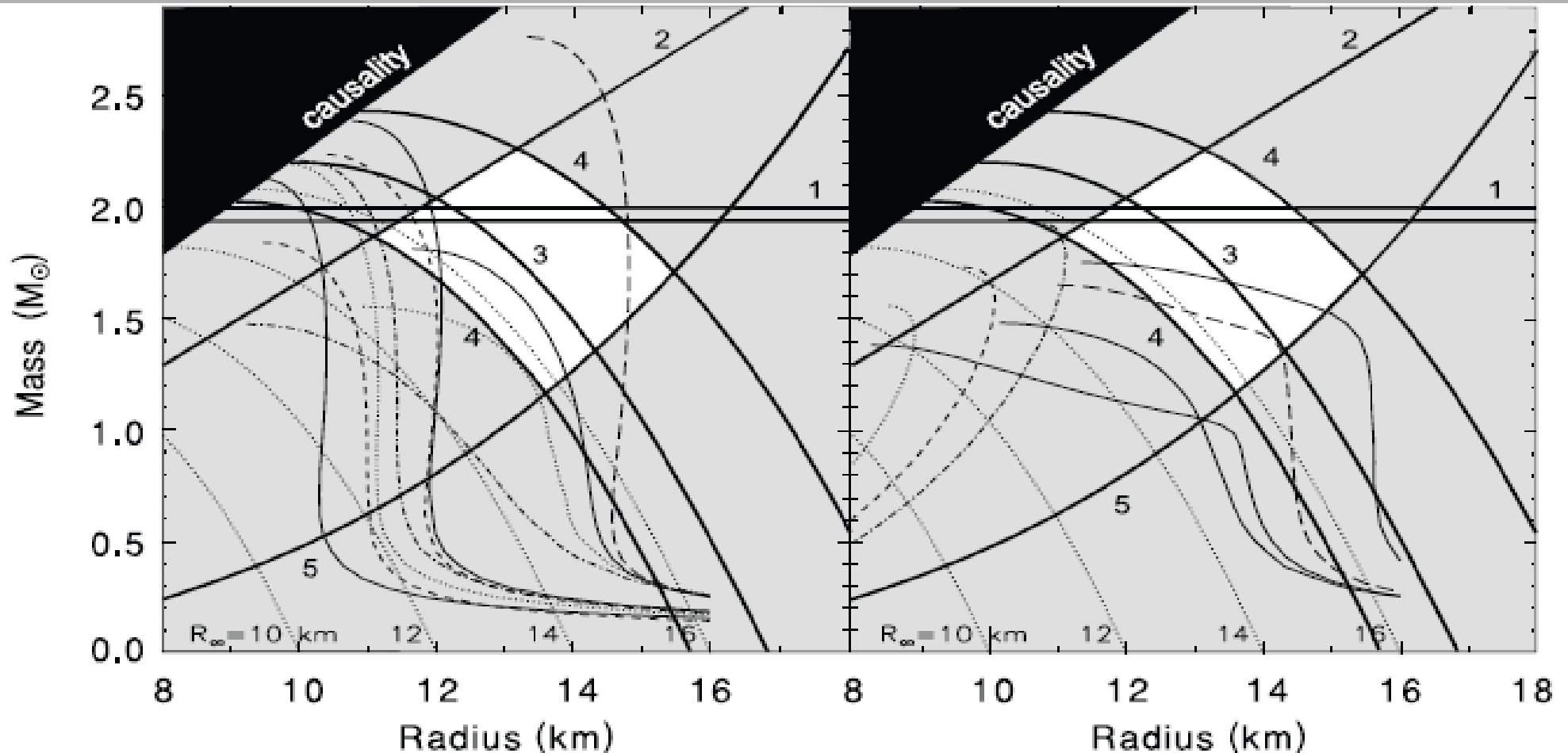
- $M_B = 1.36 M_\odot$ favors asy-soft EoS
- $\Delta M_B = 0.002 M_\odot$ equiv to $\Delta L = 20$ MeV
- lowering M_B at fixed M lowers the gravitational binding energy and increases the star radius
- what if M_B were lower ?
- $M_B = 1.355 M_\odot$ favors asy-stiff EoS !?



Compact Star Measurements

The background of the slide features several thick, light gray, wavy lines that flow from the bottom right towards the center, creating a sense of movement and depth.

Which constraints can be trusted ?



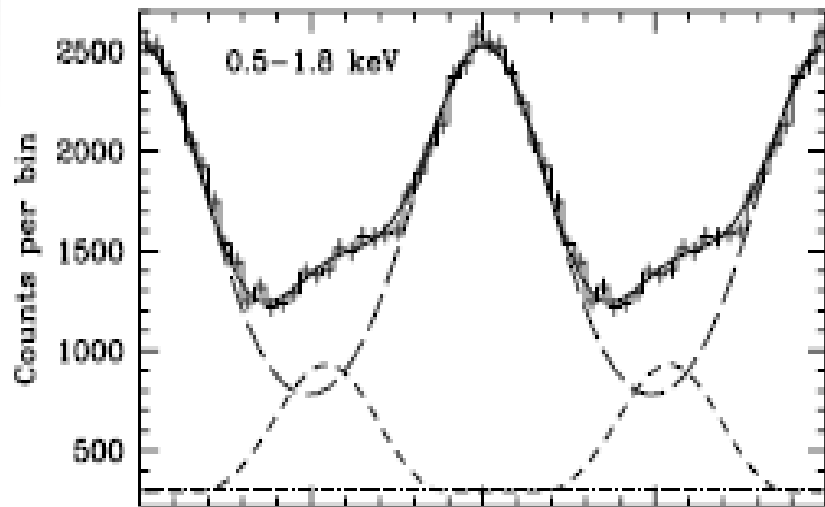
- 1 – Largest mass J1614 – 2230 (Demorest et al. 2010)
- 2 – Maximum gravity XTE 1814 – 338 (Bhattacharyya et al. (2005))
- 3 – Maximum radius RXJ 1856 – 3754 (Trumper et al. 2004)
- 4 – Radius, 90% confidence limits LMXB X7 in 47 Tuc (Heinke et al. 2006)
- 5 – Largest spin frequency J1748 – 2446 (Hessels et al. 2006)

Which constraints can be trusted ?

Nearest millisecond pulsar PSR J0437 – 4715 revisited by XMM Newton

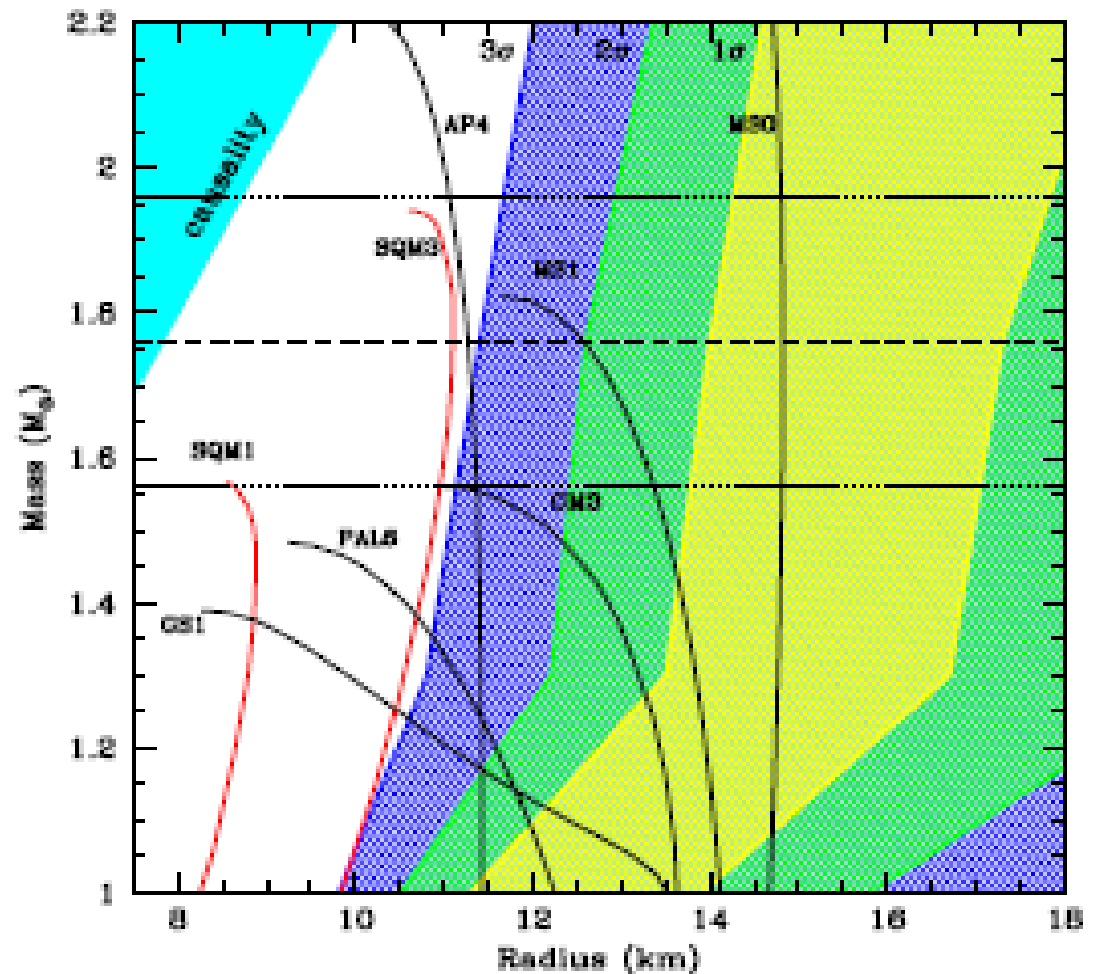
Distance: $d = 156.3 \pm 1.3$ pc

Period: $P = 5.76$ ms, $\dot{P} = 10^{-20}$ s/s, field strength $B = 3 \times 10^8$ G

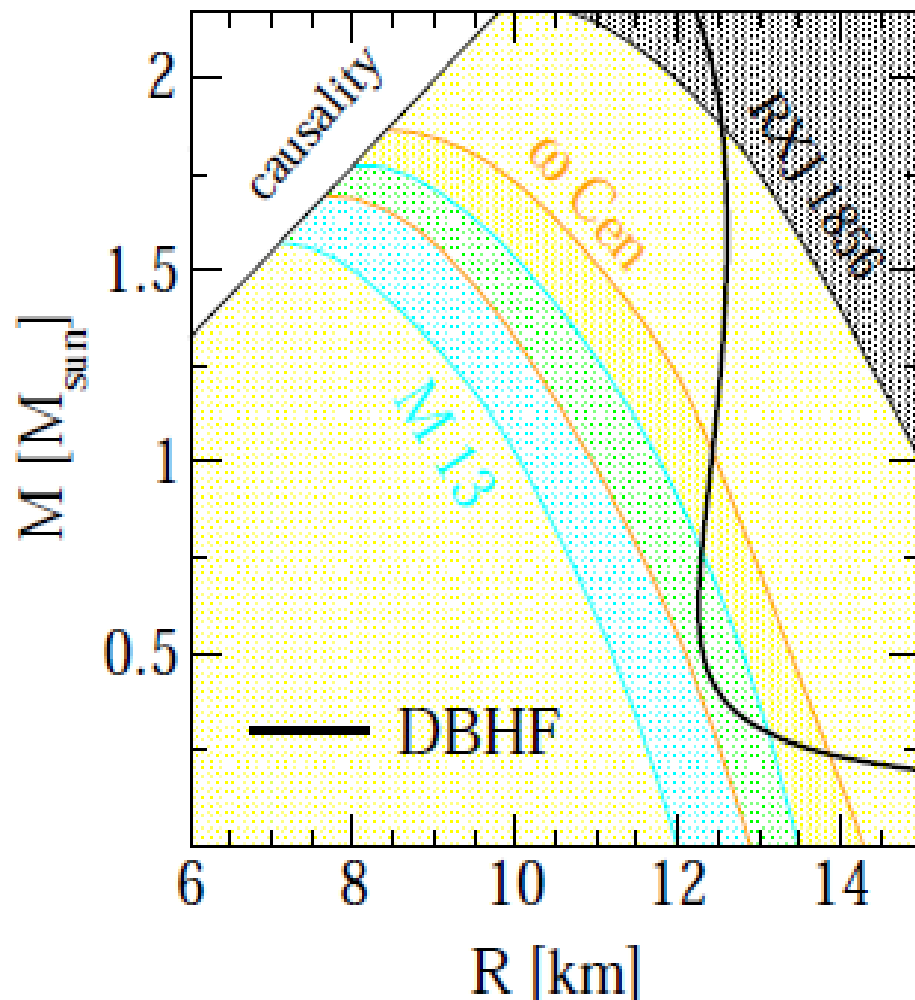


Three thermal component fit
 $R > 11.1$ km (at 3 sigma level)
 $M = 1.76 M_{\text{sun}}$

S. Bogdanov, arxiv:1211.6113 (2012)



Measure masses and radii of CS!



- Distance measured
 - Spectrum measured (ROSAT, XMM, Chandra)
 - Luminosity measured
- effective temperature T_∞
- photospheric radius

$$R_\infty = R / \sqrt{1 - R/R_S}, \quad R_S = 2GM/R$$

Object	R_∞ [km]	Reference
RXJ 1856	16.8	Trümper et al. (2004)
ω Cen	13.6 ± 0.3	Gendre et al. (2003)
M13	12.8 ± 0.4	Gendre et al. (2004)

Lower limit from RXJ 1856 incompatible with ω Cen and M13 ?

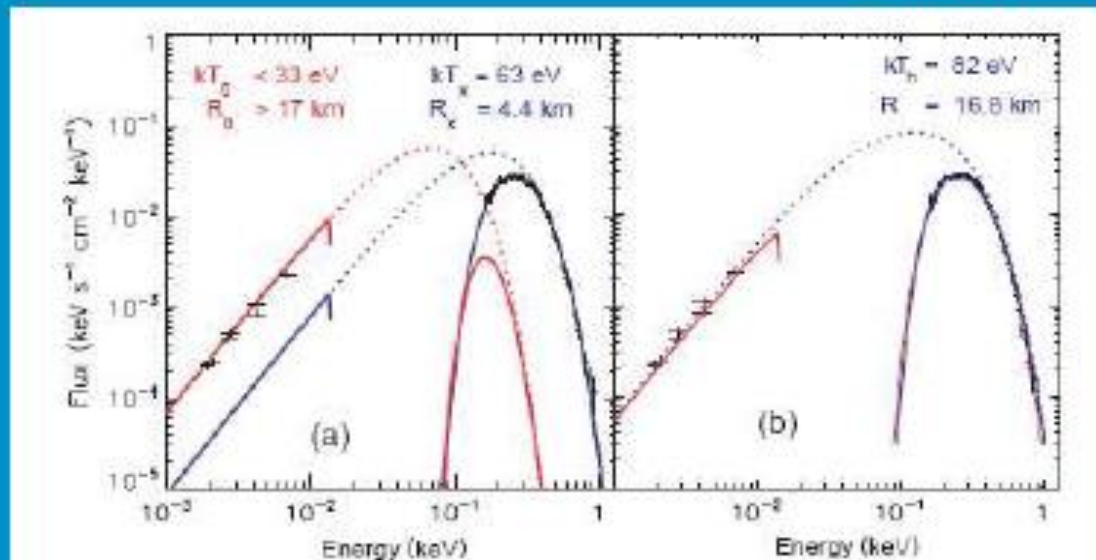
The lesson learned from RX J1856

blackbody fits to the optical and X-ray spectra of RX J1856.5-3754 (Trümper, 2004)

radius determination \Rightarrow EoS \Rightarrow state of matter at high densities

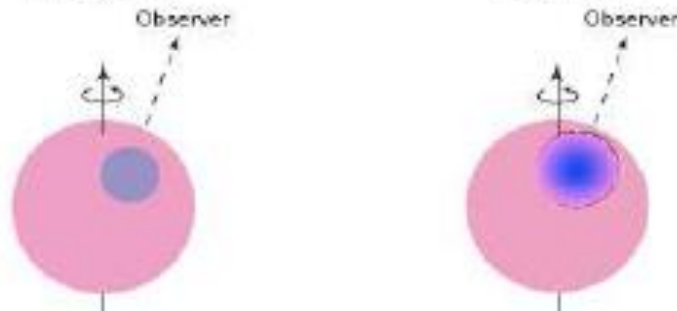
two-component model

model with continuous
T-distribution



completely featureless
X-ray spectrum:
condensed surface?
 \Rightarrow strong B?

$L_x = 5.4 \times 10^{30} \text{ erg s}^{-1}$



pulsed fraction $< 1\% \Rightarrow$
line of sight \parallel rotation axis?

X-ray emitting region is a “hot spot”, J. Trümper et al., Nucl. Phys. Proc. Suppl. 132 (2004) 560

Bayesian Analysis for the EoS

Bayesian TOV analysis:

Steiner, Lattimer, Brown, ApJ 722 (2010) 33

Most Probable Values for Masses and Radii for Neutron Stars Constrained to Lie on One Mass Versus Radius Curve

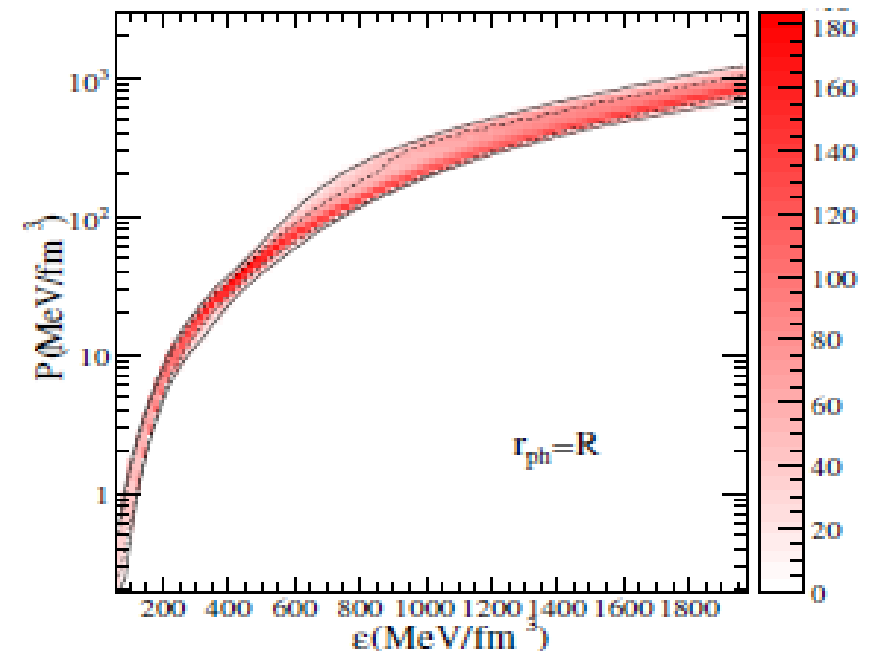
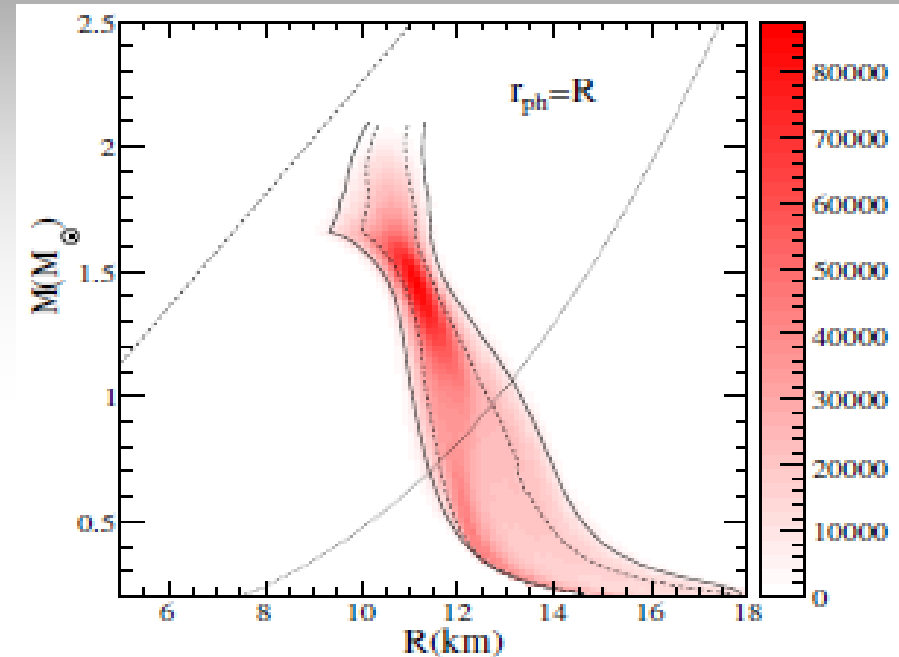
Object	$r_{\text{ph}} = R$		$r_{\text{ph}} \gg R$	
	$M (M_{\odot})$	$R \text{ (km)}$	$M (M_{\odot})$	$R \text{ (km)}$
4U 1608–522	$1.52^{+0.22}_{-0.18}$	$11.04^{+0.53}_{-1.50}$	$1.64^{+0.34}_{-0.41}$	$11.82^{+0.42}_{-0.89}$
EXO 1745–248	$1.55^{+0.12}_{-0.36}$	$10.91^{+0.86}_{-0.65}$	$1.34^{+0.450}_{-0.28}$	$11.82^{+0.47}_{-0.72}$
4U 1820–30	$1.57^{+0.13}_{-0.15}$	$10.91^{+0.39}_{-0.92}$	$1.57^{+0.37}_{-0.31}$	$11.82^{+0.42}_{-0.82}$
M13	$1.48^{+0.21}_{-0.64}$	$11.04^{+1.00}_{-1.28}$	$0.901^{+0.28}_{-0.12}$	$12.21^{+0.18}_{-0.62}$
ω Cen	$1.43^{+0.26}_{-0.61}$	$11.18^{+1.14}_{-1.27}$	$0.994^{+0.51}_{-0.21}$	$12.09^{+0.27}_{-0.66}$
X7	$0.832^{+1.19}_{-0.051}$	$13.25^{+1.37}_{-3.50}$	$1.98^{+0.10}_{-0.36}$	$11.3^{+0.95}_{-1.03}$

Caution:

If optical spectra are not measured, the observed X-ray spectrum may not come from the entire surface
But from a hot spot at the magnetic pole!

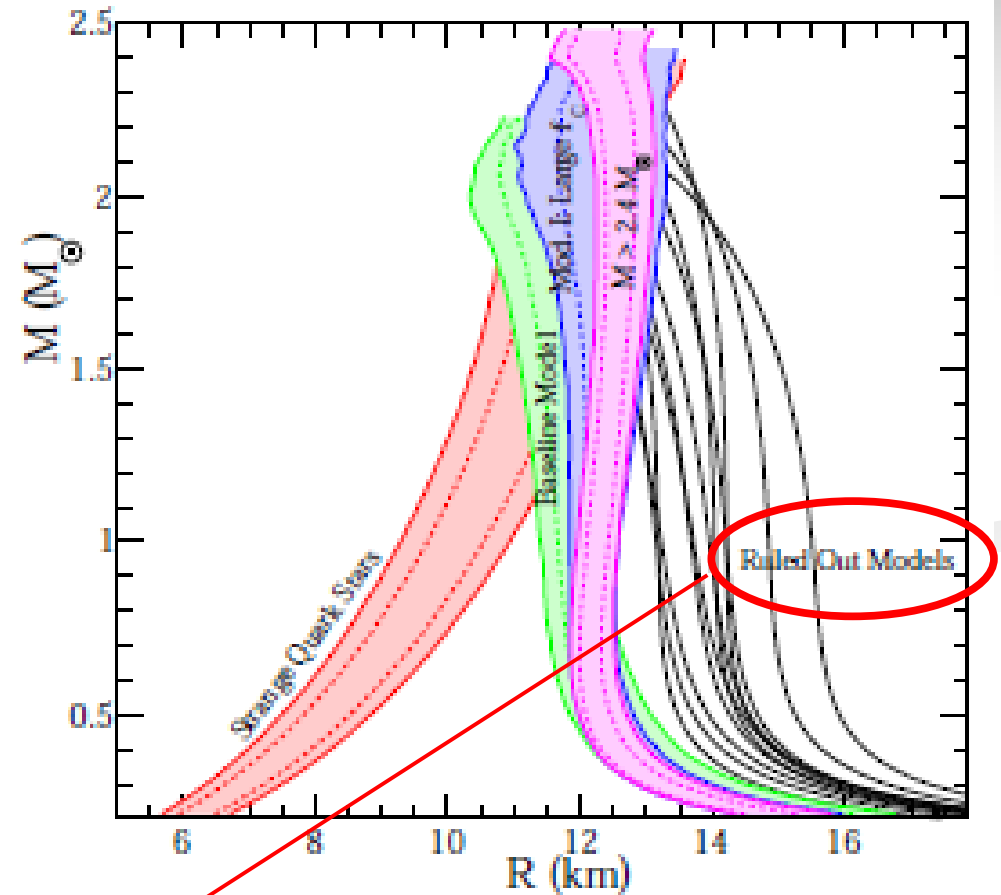
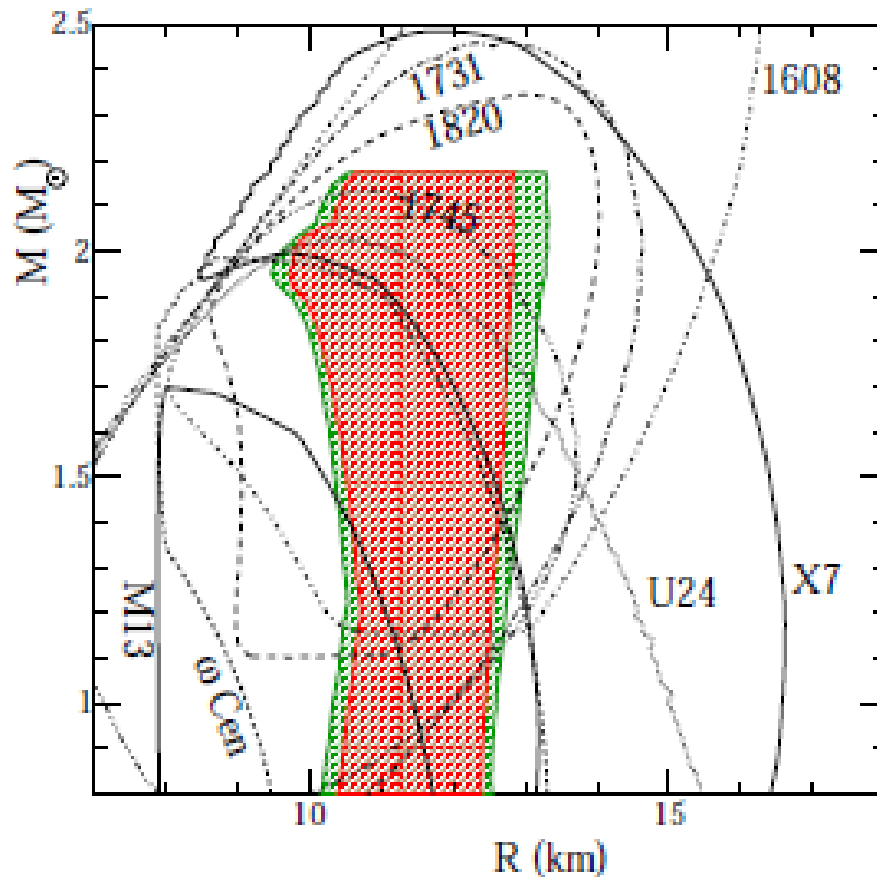
J. Trumper, Prog. Part. Nucl. Phys. 66 (2011) 674

Such systematic errors are not accounted for in Steiner et al. $\rightarrow M(R)$ is a lower limit \rightarrow softer EoS



Which constraints require caution ?

A. Steiner, J. Lattimer, E. Brown, ApJ Lett. 765 (2013) L5



“Ruled out models” - too strong a conclusion!

$M(R)$ constraint is a lower limit, which is itself included in that from RX J1856, which is one of the best known sources.

Bayesian Analysis

The background of the slide features several light gray, wavy, horizontal lines that sweep across the bottom right portion of the frame, creating a sense of motion and depth.

Bayesian Analysis

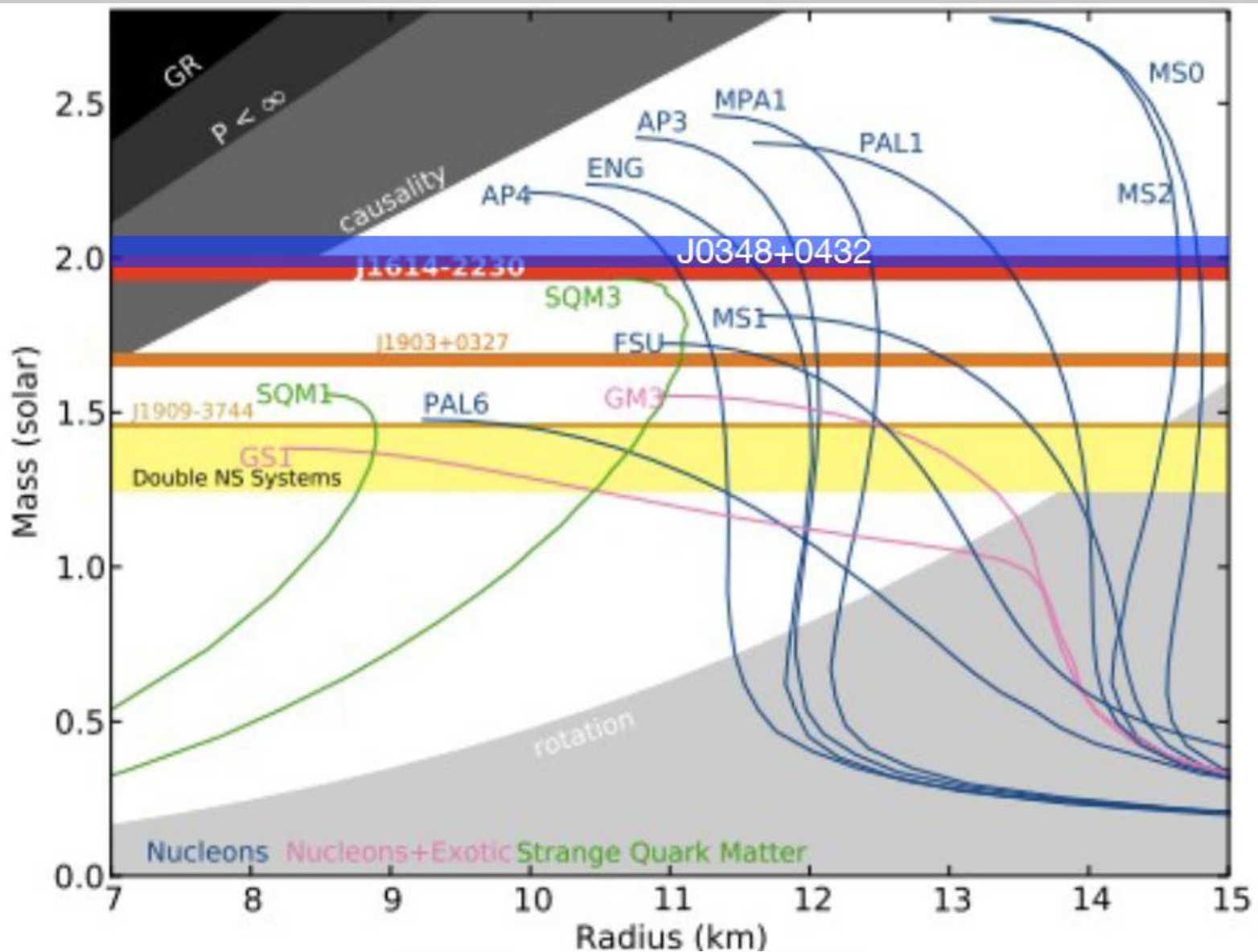
Note, that these measurements are independent of each other. This means that we can calculate the complete conditional probability of an event E given π_i corresponds to the product of the conditional probabilities of all measurements, in our case resulting from the three constraints E_A, E_B, E_K ,

$$P(E|\pi_i) = P(E_A|\pi_i) \cdot P(E_B|\pi_i) \cdot P(E_K|\pi_i). \quad (17)$$

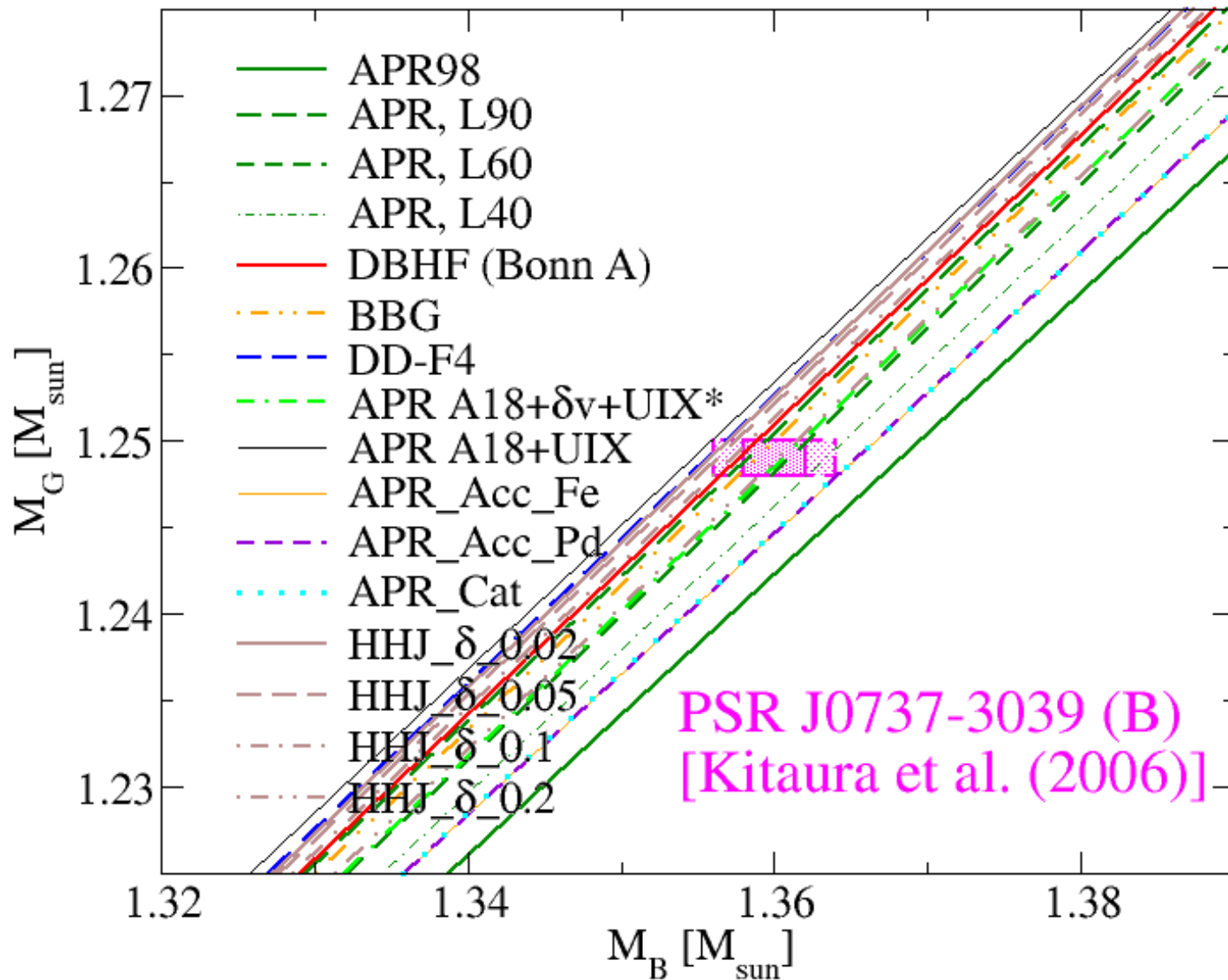
Now, we can calculate the probability of π_i using Bayes' theorem:

$$P(\pi_i|E) = \frac{P(E|\pi_i) P(\pi_i)}{\sum_{j=0}^{N-1} P(E|\pi_j) P(\pi_j)}. \quad (18)$$

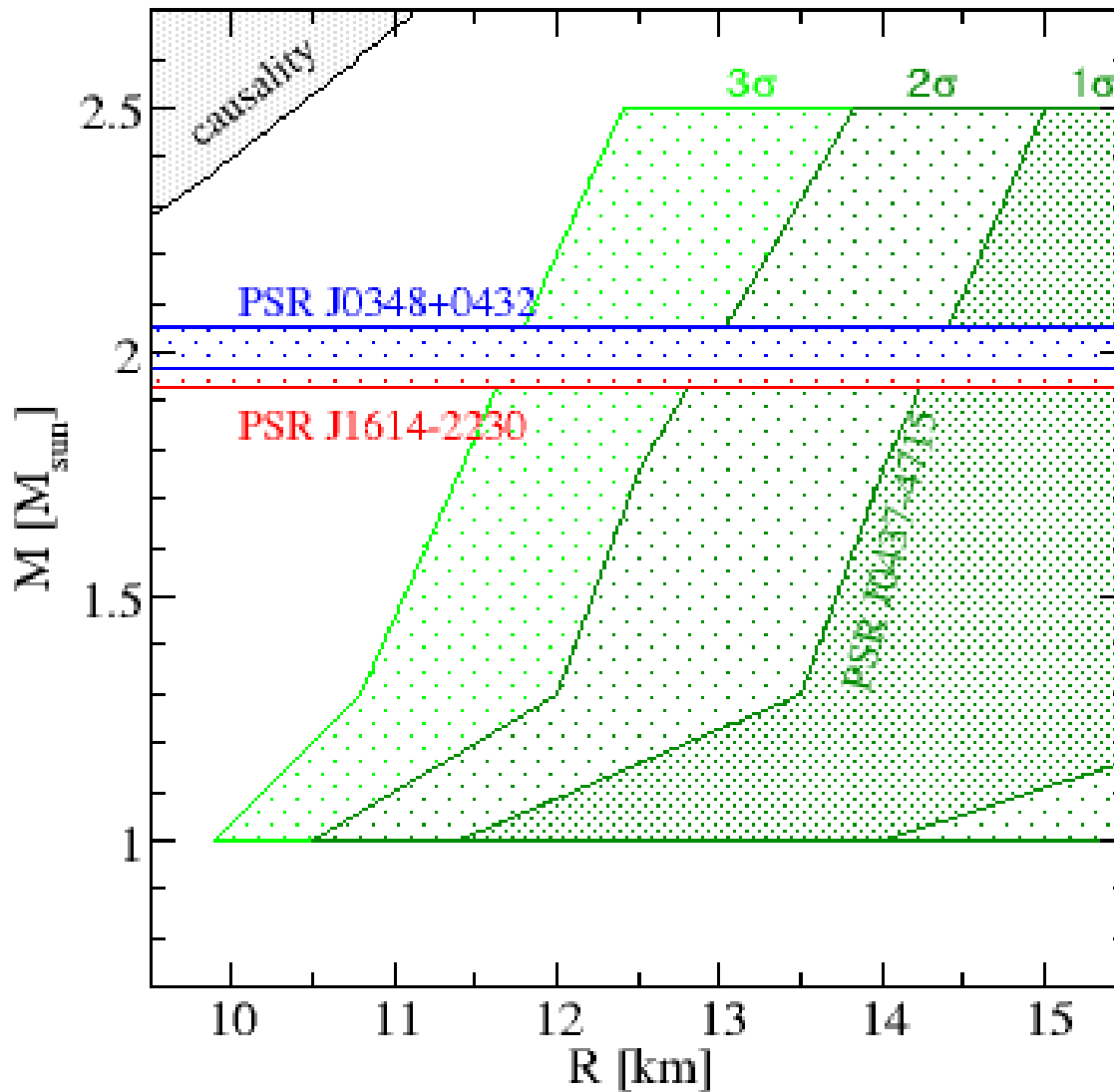
Mass vs. Radius Relation



Baryonic Mass



Mass-radius Constraints



EoS parameterization

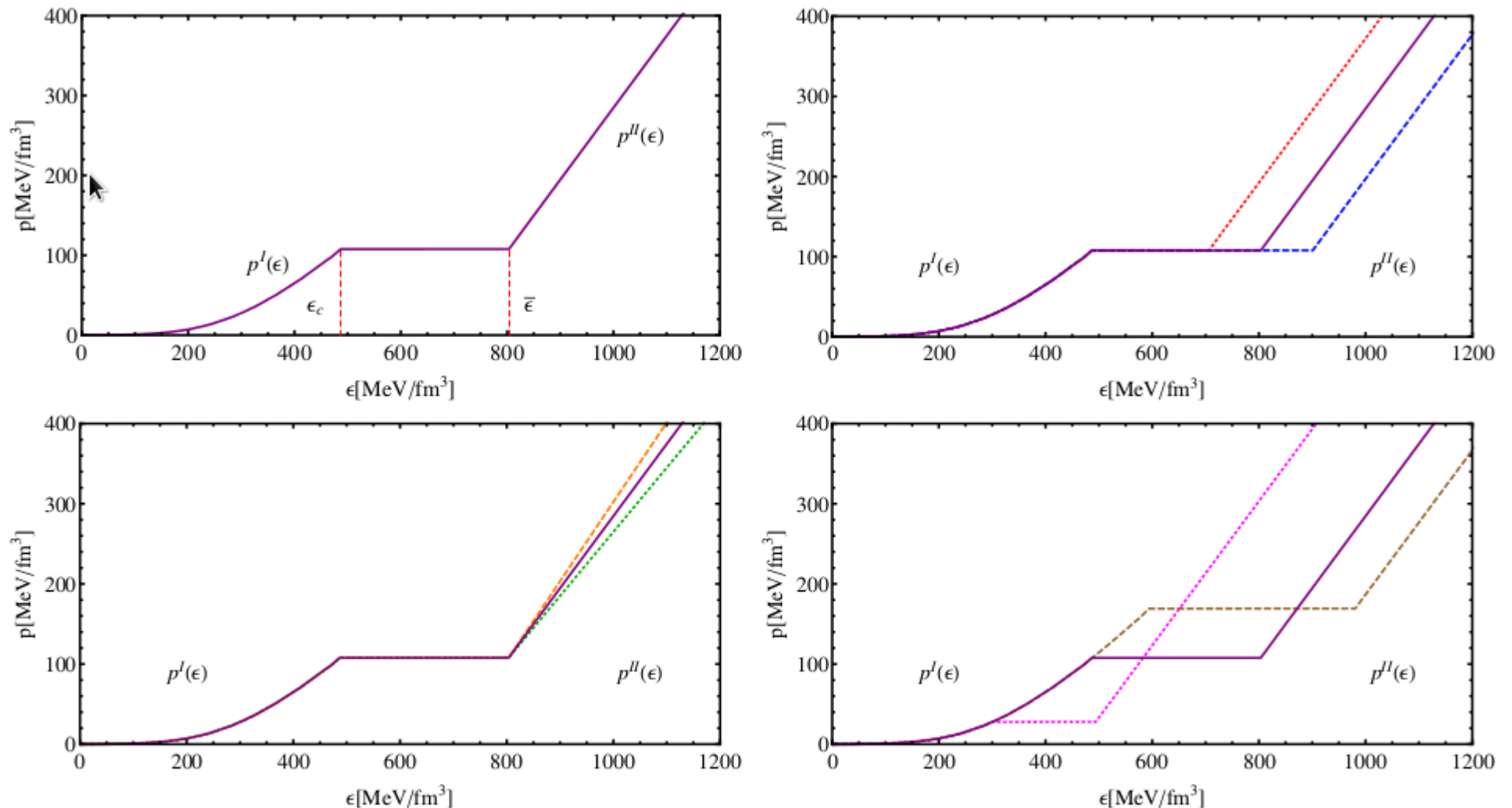
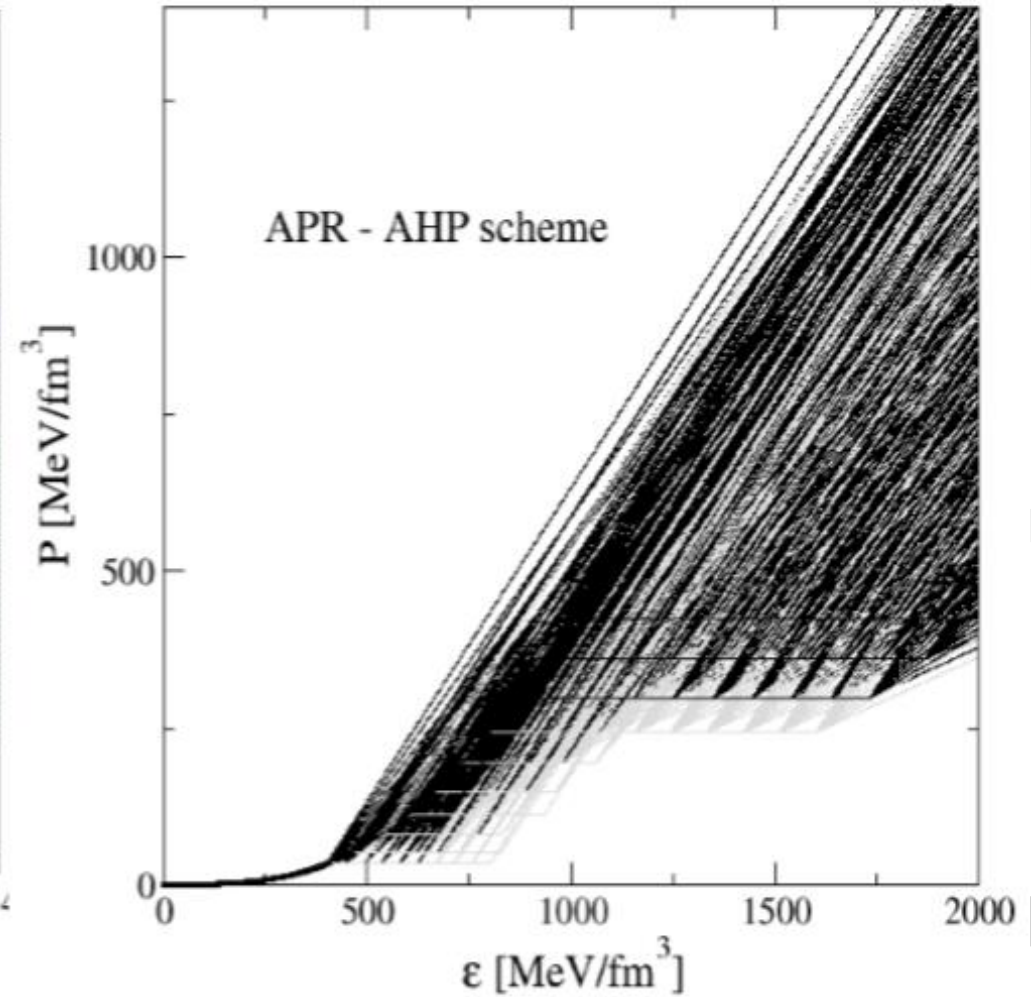
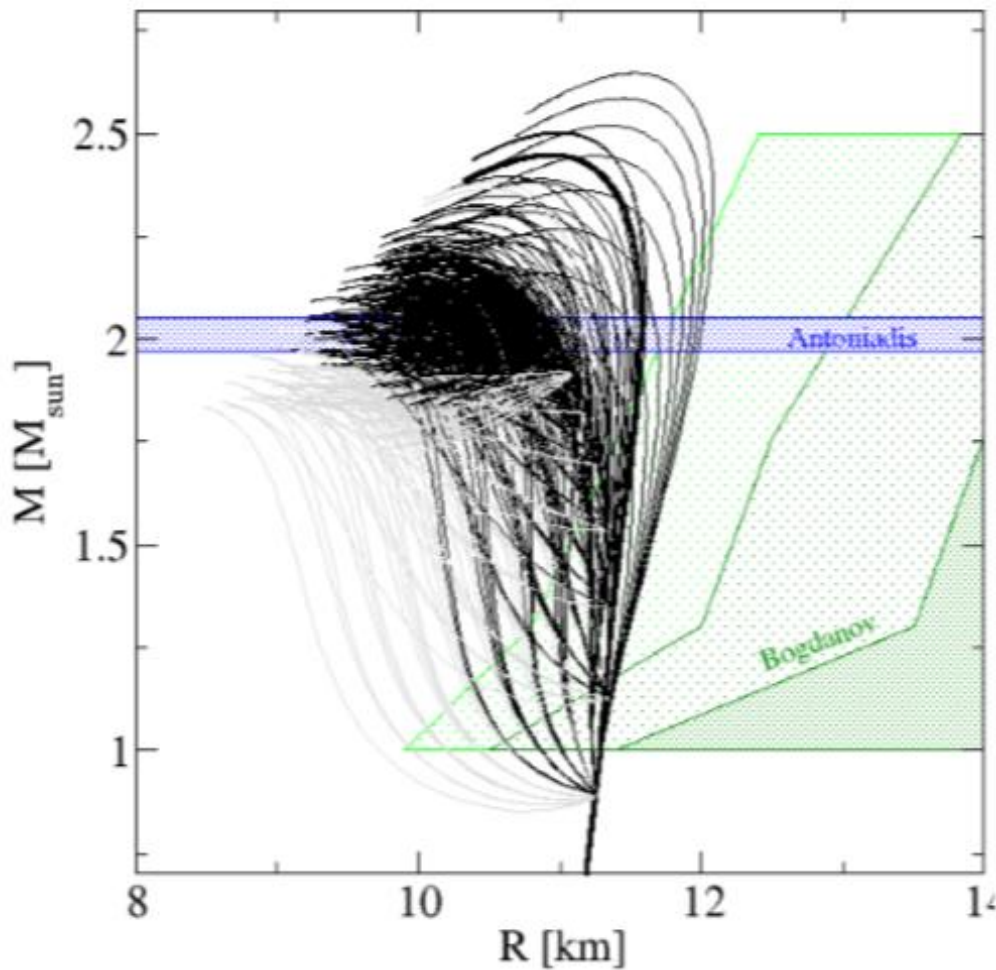


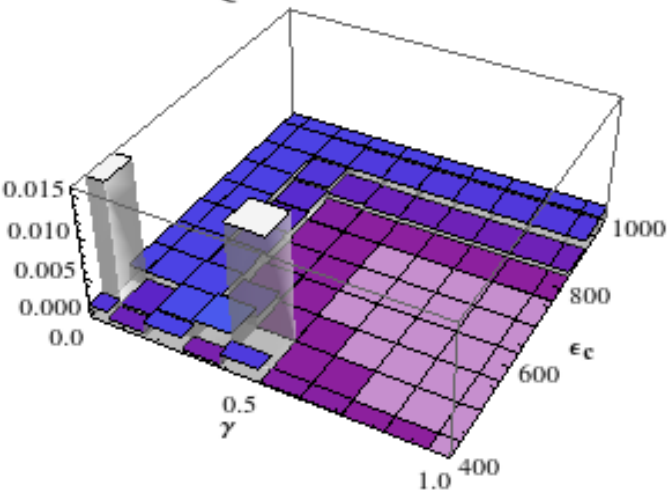
FIG. 2: Hybrid EoS scheme for two sets of parameters. *Upper left corner:* EoS with parameters $\epsilon_c = 446.966$ MeV/fm³, $c_{QM}^2 = 0.9$ and $\Delta\epsilon/\epsilon_c = 0.65$ used as a reference for the rest of the figures. *Upper right corner:* $\Delta\epsilon/\epsilon_c = 0.45$ (dotted), $\Delta\epsilon/\epsilon_c = 0.85$ (dashed) modified parameters in these EoS. *Lower left corner:* $c_{QM}^2 = 0.8$ (dotted) $c_{QM}^2 = 0.99$ (dashed) modifications. *Lower right corner:* $\epsilon_c = 299.359$ MeV/fm³ (dotted) and $\epsilon_c = 594.276$ MeV/fm³ (dashed) changes in these EoS with respect to the original.

Disjunct M-R constraints for Bayesian analysis !

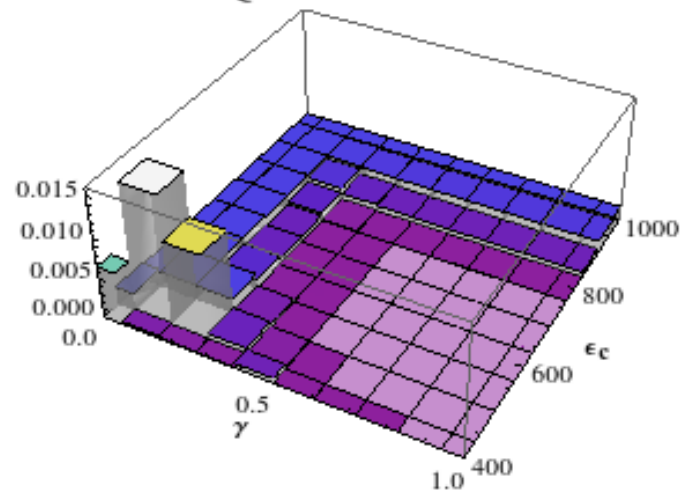


Posterior probabilities (highest values)

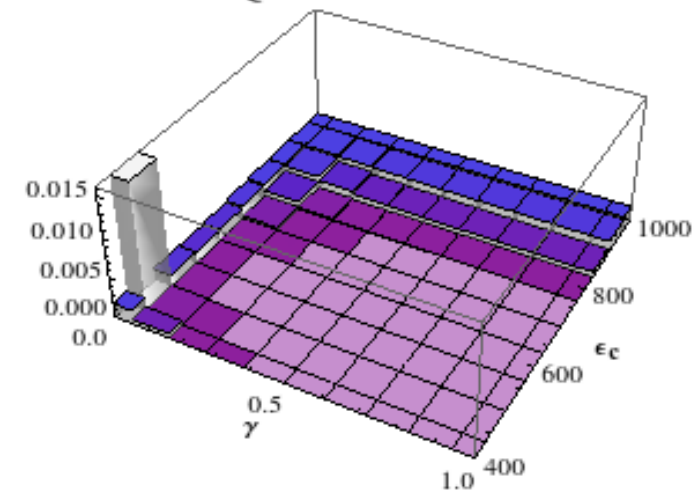
$$c^2_{QM}=0.922222$$



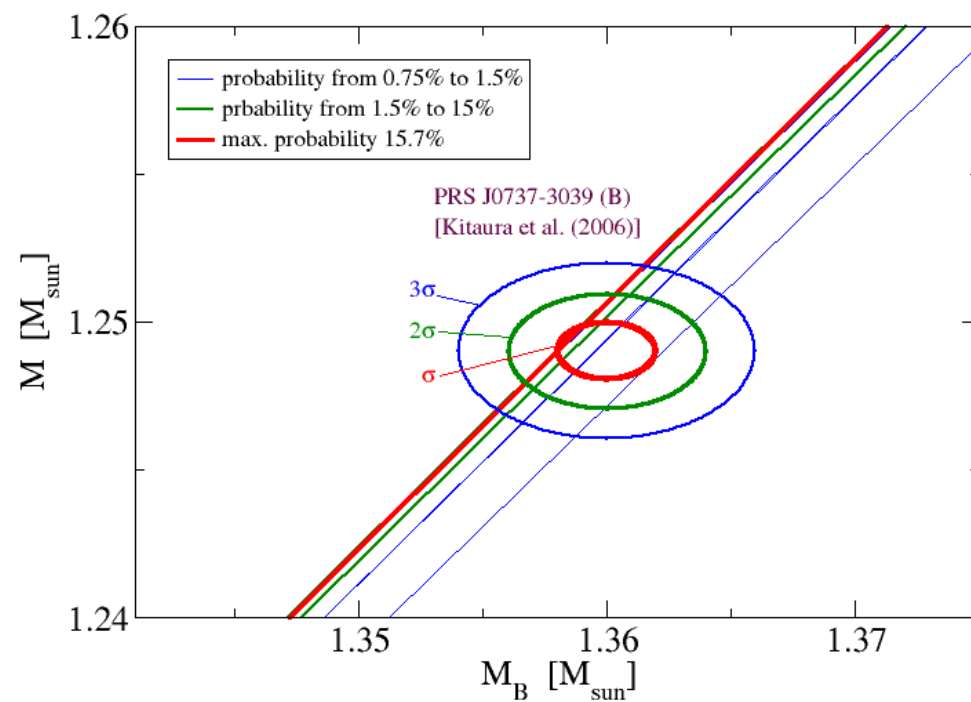
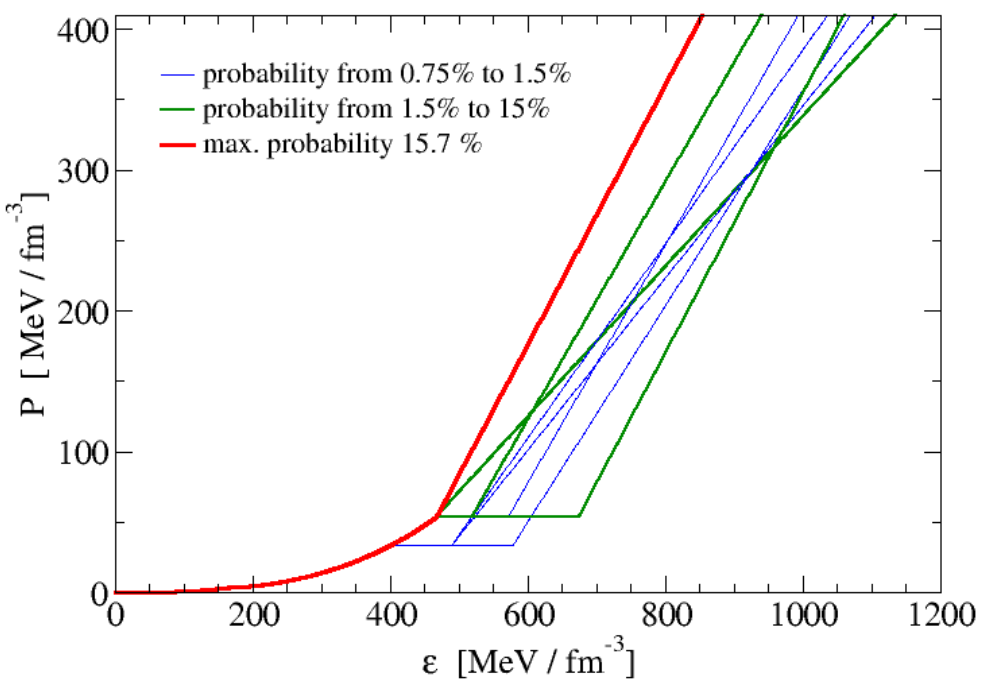
$$c^2_{QM}=0.844444$$



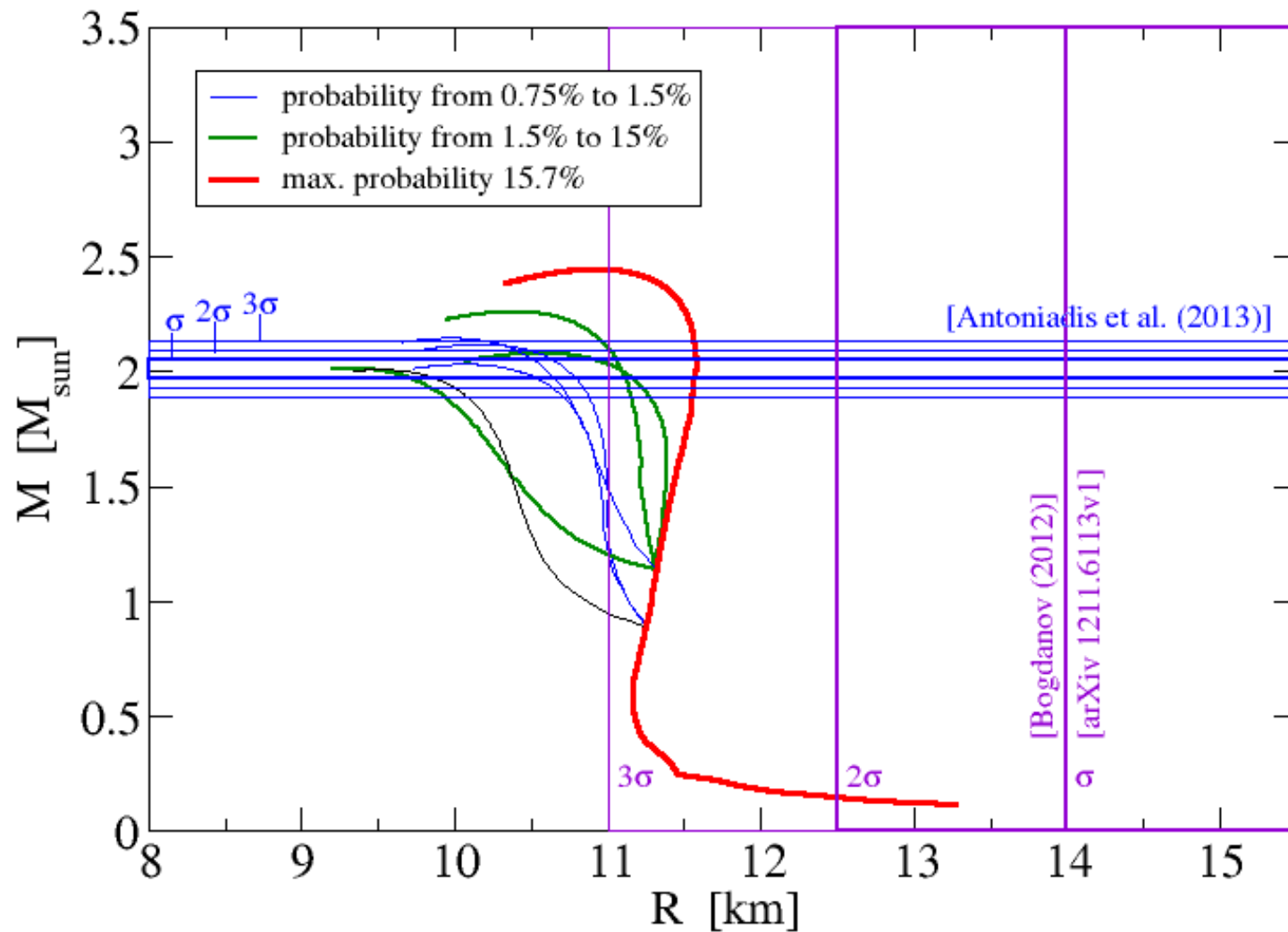
$$c^2_{QM}=0.533333$$



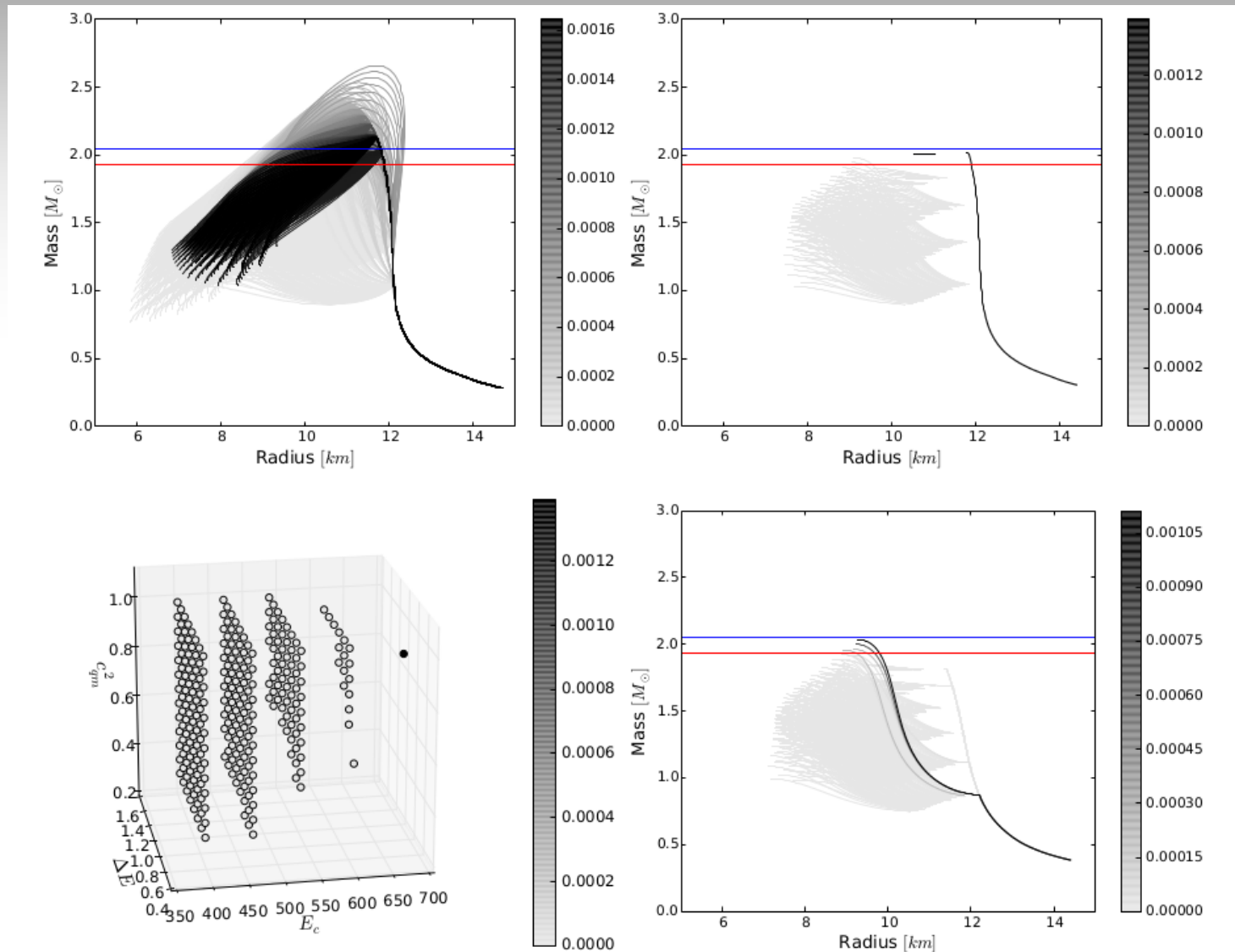
The most probable EoS set



The most probable EoS set



Phase transition measuring radii



Alvarez-Castillo, Ayriyan, Blaschke, Grigorian, Sokolowski (in progress, 2014)

Conclusions

- Given the knowledge from lattice QCD that at zero baryon density the QCD phase transition proceeds as a crossover, twins would then support the existence of a CEP in the QCD phase diagram.
- Modelling compact star twins is possible via realistic models based on a QCD motivated hNJL models fulfilling observations.
- Bayesian Analysis on hybrid compact star EoS has the power to provide the corresponding probabilities for radius measurements in order to identify mass twins.

GRACIAS